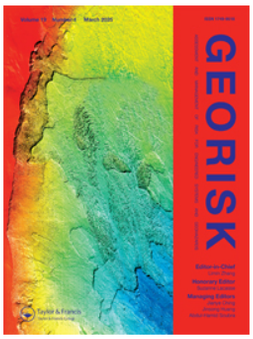

Taylor & Francis
Taylor & Francis Group

Georisk: Assessment and Management of Risk for Engineered Systems and Geohazards

ISSN: (Print) (Online) Journal homepage: www.tandfonline.com/journals/ngrk20

Quantifying the effects of vibro-compaction on soil heterogeneity and geotechnical uncertainty

Martí Lloret-Cabot, Kun Zhang, Wangcheng Zhang, Alaa Kourdey & Michael A. Hicks

To cite this article: Martí Lloret-Cabot, Kun Zhang, Wangcheng Zhang, Alaa Kourdey & Michael A. Hicks (21 Mar 2025): Quantifying the effects of vibro-compaction on soil heterogeneity and geotechnical uncertainty, Georisk: Assessment and Management of Risk for Engineered Systems and Geohazards, DOI: 10.1080/17499518.2025.2478636

To link to this article: https://doi.org/10.1080/17499518.2025.2478636

Published online: 21 Mar 2025.

GEORISK
https://doi.org/10.1080/17499518.2025.2478636

Taylor & Francis
Taylor & Francis Group

Quantifying the effects of vibro-compaction on soil heterogeneity and geotechnical uncertainty

Martí Lloret-Cabot[a], Kun Zhang[a], Wangcheng Zhang[a], Alaa Kourdey[a] and Michael A. Hicks[b]

[a]Department of Engineering, Durham University, Durham, UK; [b]Department of Geoscience & Engineering, Delft University of Technology, Delft, the Netherlands

ABSTRACT

Geological materials exhibit spatial variability in their properties as a result of their formation. Many studies have focussed on how to characterise this spatial variation by means of the correlation length θ. Such a characterisation has been applied in the geotechnical design of geostructures at numerous sites where cone penetration tests (CPTs) were available, because θ can be relatively easily estimated from this in-situ information. However, the CPTs available at a given site are often part of the initial site investigation, and hence carried out before the application of any ground improvement technique. This raises the question of how (and by how much) the estimated θ is affected by subsequent stages of the construction project and, more specifically, by the application of ground improvement processes intended to alter the initially poor mechanical condition of the in-situ soil. This paper investigates in-situ data from three trial test sites, where CPT data before and after application of vibro-compaction are available. In addition to the expected overall mechanical improvement of the soil, the application of vibro-compaction has a significant impact on soil heterogeneity, with a substantial reduction in the coefficient of variation and θ of the cone tip resistance and sleeve friction.

ARTICLE HISTORY
Received 17 June 2024
Accepted 8 March 2025

KEYWORDS
cone penetration test; correlation length; scale of fluctuation; soil spatial variability; vibro-compaction

1. Introduction

Soils are naturally heterogeneous as a consequence of their formation and subsequent geological/geotechnical history. A knowledge of the extent of the spatial (i.e. within a soil layer) and temporal (i.e. over their lifetime) variations of their geotechnical properties is important for the design of geotechnical structures. Commonly, the relevance of the random temporal variations of a soil property is of less interest to geotechnical engineers than its random variation in the spatial dimension, which may explain why the random temporal nature of soil properties are less often taken into account. However, many geotechnical projects require the application of ground improvement techniques (e.g. vibro-compaction) to improve the originally poor mechanical and hydrological properties of the in-situ ground (Baumann and Bauer 1975) and these techniques are typically applied after carrying out an initial in-situ soil characterisation. The sequence of these construction stages raises the question of how, and by how much, such ground improvement techniques influence the heterogeneity of the soil profile, and what are the likely implications for the reliability-based design of a geotechnical structure.

Alonso and Krizek (1975) and Vanmarcke (1983) demonstrated that the spatial variation of a soil property can be relatively well described by means of an important spatial statistic referred to as the spatial correlation length (or scale of fluctuation) θ. This spatial statistic controls the decay of the spatial correlation structure of a soil property with distance (in a given direction). The estimation of θ has been extensively discussed in the geotechnical literature (Baecher and Christian 2005; Campanella, Wickremesinghe, and Robertson 1987; Ching et al. 2023; Ching, Phoon, and Sung 2017; DeGroot and Baecher 1993; Fenton et al. 2015; Hicks and Samy 2002; Li et al. 2021; Lloret-Cabot, Hicks, and van den Eijnden 2012; Phoon and Kulhawy 1999; Popescu, Deodatis, and Nobahar 2005; Uzielli et al. 2007; Uzielli, Vannucchi, and Phoon 2005; Wackernagel 2003). The initial focus was correlation in the vertical direction (Cafaro and Cherubini 2002; de Gast, Vardon, and Hicks 2017; Lloret-Cabot, Hicks, and Nuttall 2013; Wickremesinghe and Campanella 2020; Zhang et al. 2021), but later also included correlation in the

CONTACT Martí Lloret-Cabot marti.lloret-cabot@durham.ac.uk Department of Engineering, Durham University, Lower Mountjoy, South Rd, Durham DH1 3LE, UK

horizontal direction (Cami et al. 2020; Ching et al. 2018; Dasaka and Zhang 2012; de Gast 2020; de Gast et al. 2021; Firouzianbandpey et al. 2014; Jaksa, Kaggwa, and Brooker 1999; Kim and Santamarina 2008; Lacasse and Nadim 1997; Larsson, Stille, and Olsson 2005; Li et al. 2014; Li, Uzielli, and Cassidy 2015; Liu et al. 2019; Lloret-Cabot, Fenton, and Hicks 2014; Monforte 2024; Onyejekwe, Kang, and Ge 2016; Pieczyńska-Kozłowska, Chwała, and Puła 2023; Stuedlein et al. 2012; Zhang et al. 2022). A detailed literature review on correlation length, including an exhaustive data base of estimated values is provided in Ching and Schweckendiek (2021).

The spatial correlation length θ is a key input parameter of numerous random field generators, such as the local average subdivision (LAS) method proposed by Fenton and Vanmarcke (1990), because it controls the representation of a soil's inherent variability within the generated random soil domain. The combination of random field theory (e.g. LAS) with the finite element method forms the so-called random finite element method (RFEM). The RFEM allows for the investigation of spatially variable soil behaviour in classical geotechnical problems (Cassidy, Uzielli, and Tian 2013; de Gast et al. 2021; de Gast, Vardon, and Hicks 2021; Fenton and Griffiths 2002, 2003, 2008, 2010; Griffiths and Fenton 1993, 2001, 2004; Griffiths, Huang, and Fenton 2009, 2011; Hicks and Onisiphorou 2005; Hicks and Spencer 2010; Hicks, Nuttall, and Chen 2014; Jiang et al. 2022; Li et al. 2022; Phoon 2008; Pieczyńska-Kozłowska and Vessia 2022; Vessia et al. 2009) and facilitates probabilistic assessments of geotechnical systems (as opposed to conventional deterministic analyses that lead to a single factor of safety). Therefore, good estimates of θ (i.e. that are representative of actual ground conditions) are critical to the application of RFEM in reliability assessments of geotechnical structures, because its value influences the averaging of properties along potential failure planes affecting the mechanical performance of the geotechnical structure investigated, as well as its probabilistic characterisation, as discussed in more detailed in Ching et al. (2018).

A number of studies in the literature have investigated and demonstrated the effectiveness of vibro-compaction on granular soils (Baumann and Bauer 1975; Lees, King, and Mimms 2013; Renton-Rose, Bunce, and Finlay 2000; Slocombe, Bell, and Baez 2000), but they mostly focused on the geotechnical improvement of the in-situ ground in terms of stiffness, strength, hydraulic conductivity and reduction of liquefaction potential. The evaluation of such soil improvement is commonly carried out by assessing cone penetration tests (CPTs) performed before (pre-) and after (post-) application of vibro-compaction. With few exceptions (Cai et al. 2017; Schorr, Cudmani, and Nübel 2023; Zhai et al. 2024), the effect that vibro-compaction has on the heterogeneity of granular deposits is rarely investigated and, to the authors' knowledge, it has not yet been investigated for sand deposits in Eastern Saudi Arabia. Filling this gap is one of the purposes of this paper. Surprisingly, studies on the characterisation of the geotechnical properties of sands from Eastern Saudi Arabia are relatively uncommon in the geotechnical literature, despite the rapid expansion and substantial investment that the region is experiencing in the construction of major infrastructure. The CPTs and the geostatistical study provided in this paper address, at least partially, this gap.

More specific aims of the paper are to quantify the heterogeneity of this Arabian sandy soil in its natural condition, in terms of the dispersion and spatial variability of cone tip resistance q_c and sleeve friction, f_s, and to then compare it with the heterogeneity of the same granular deposits after the application of vibro-compaction. Such a comparison enables the expected benefits of vibro-compaction on the overall increased means of both soil properties to be confirmed, as well as quantifying the lesser known effect that vibro-compaction has on the point variances (and associated histograms) of these properties. In addition, the study facilitates a comparison of their spatial variability (vertical and horizontal) before and after vibro-compaction to quantify the impact of this ground improvement method; something that is currently unknown for these soils. Finally, the overall study on the heterogeneity will provide a valuable source of information, not only to anticipate the potential benefits of vibro-compaction at similar sites in the region, but also as an additional way of assessing quality in the execution of this ground improvement method.

For this investigation, in-situ CPT data from a large construction project in Saudi Arabia have been used to geo-statistically characterise the state of sand deposits at the site. This was done in terms of the point statistics (i.e. mean μ, variance σ^2 and coefficient of variation CoV), probability density function (pdf) and spatial statistics (i.e. correlation lengths in the vertical θ_v and horizontal θ_h directions) of both the measured CPT tip resistances, q_c, and sleeve frictions, f_s, before (pre-) and after (post-) application of vibro-compaction. Importantly, three trial sites have CPT data available before and after vibro-compaction. This allowed for a thorough quality assessment, which included the proposal, by the engineering contractor responsible for the ground improvement works, of an *acceptance criterion* to ensure that minimum target values of q_c were achieved at

different specified depths of the granular deposits after vibro-compaction. However, the data are herein used for the statistical quantification and analysis of the effect that vibro-compaction has on soil heterogeneity and the associated geotechnical uncertainty.

2. Statistical soil characterisation of the site

A shipyard is in the final stages of construction in the Eastern Province of Saudi Arabia, covering an area of about 1,125 ha. Because of its very large extent, an extensive quality assurance and monitoring programme was carried out before and during construction. Based on the information from the drilled boreholes, the predominant ground conditions across the site were identified to be deposits of saturated medium dense to dense calcareous sands, with occasional bands of calcarenite caprock, overlying weak calcareous sandstone and siltstone at approximately 20 m below the ground surface. A typical CPT profile from the site is illustrated in Figure 1, including the tip resistance q_c, sleeve friction f_s and pore water pressure u_w. The figure shows that the phreatic surface is at the ground surface and that the variation of u_w with depth is approximately hydrostatic. It also shows that the measured tip resistances are quite variable within the first few metres below the ground surface, reaching substantially high values (up to about 40 MPa). As further discussed later, these very large tip measurements near the ground surface are explained by the presence of a superficial thin layer of sand dry crust and interbedded thin layers of stronger material at shallow depths (e.g. calcarenite caprock). Complementary geotechnical information on representative properties of similar sand deposits in the area can be found elsewhere (Poulos 2018).

Of the total projected area of the shipyard, this research focusses on three representative smaller areas referred to as trial test sites A, B and C. Each of these trial sites has a plan area of about 30 m × 30 m, as illustrated in Figure 2. The figure shows the locations where vibro-compaction was applied (referred to as print points) and the locations of all CPTs before and after vibro-compaction. Nine CPT soundings are available for trial sites A and B. From these sites, four CPTs are available from before the application of vibro-compaction, which will be referred to as pre-CPTs hereafter (and are indicated as A1-A4 and B1-B4). Four further CPTs were executed 50 days after vibro-compaction at each of these sites, at 1 m distance from the corresponding pre-CPT to reduce the influence of distance between the two CPT readings (see Figure 2). These are referred to as post-CPTs (A1-A4 and B1-B4). Test trial site C has

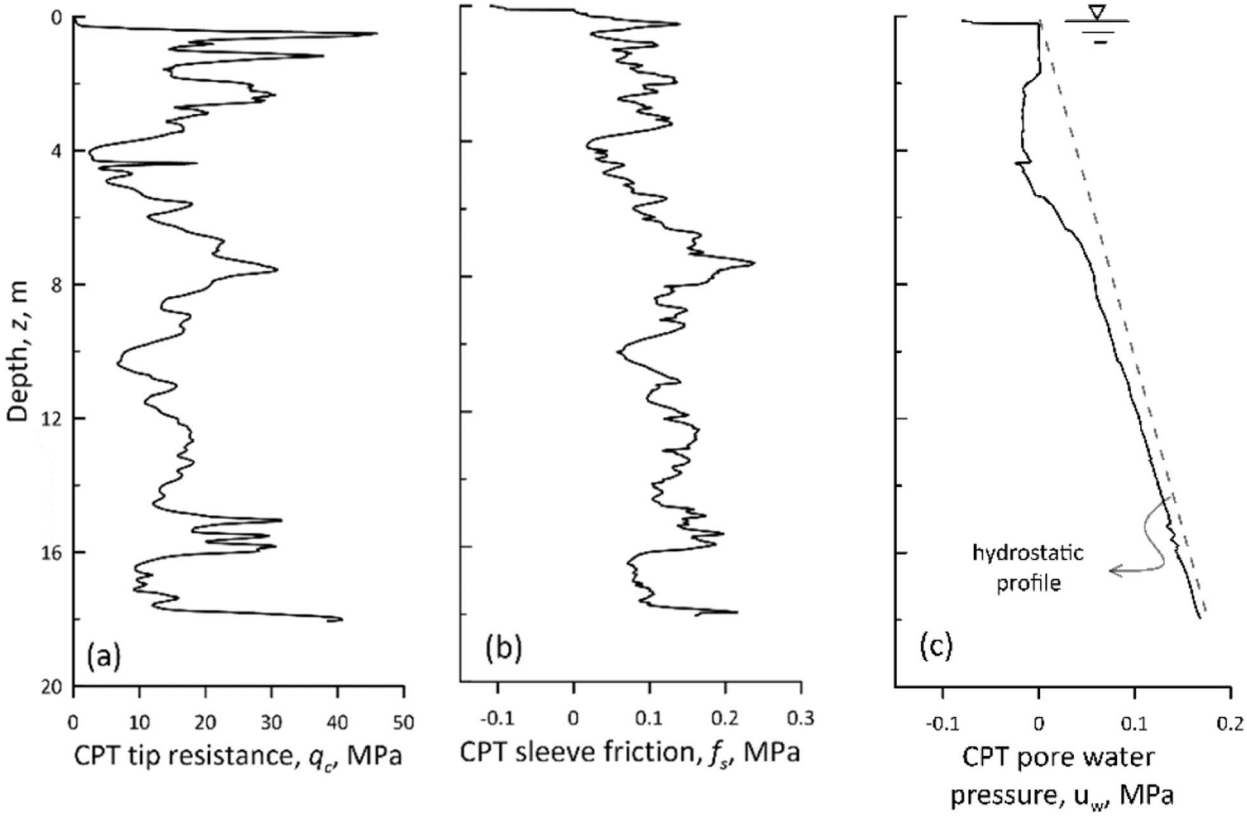

Figure 1. Typical CPT soil profile: (a) tip resistance; (b) sleeve friction and (c) pore water pressure.

eleven CPTs: five pre-CPTs and five post-CPTs (C1-C5). One additional CPT was carried out 10 days after the post-CPTs at sites A, B and C to check the overall mechanical improvement of the soil after vibro-compaction (denoted as T-A, T-B and T-C, respectively).

Vibro-compaction is typically used in cohesionless soils (as in this construction project) because denser configurations of their granular arrangement can be easily attained by the application of vibration, especially if the soils are initially in a loose state. Indeed, the application of vibro-compaction in coarse-grained soils results in a reduced void ratio and compressibility, increased strength (higher friction angle) and increased seismic resistance (Slocombe, Bell, and Baez 2000). Application of vibro-compaction at the trial areas was performed according to project specifications. These involved setting out first the locations of the pre-CPTs at each trial area, with a frequency of at least one CPT per 200 m^2 of plan area (see Figure 2). To achieve a more uniform densification of the sand state with depth, the vibration is applied in stages, starting in this project from a depth of about 15 m and then raising the vibrator to the desired new level in 1 m lift intervals. Each stage requires the vibrator to be maintained for a specified time (i.e. holding time or period), which was here set to between 30 and 40 s. The densification effect tends to reduce with depth and, at any given depth, densification decreases with increasing radius from the vibrator (Slocombe, Bell, and Baez 2000). This means that, in addition to specifying a lift interval and holding time, it is also necessary to establish a plan grid. The design of the adopted plan grid is shown in Figure 2 for the two triangular grids considered in this construction project. One denser grid was formed from approximately equilateral triangles of side length 3.6 m and resulted in about 20 prints, while another less dense grid of slightly

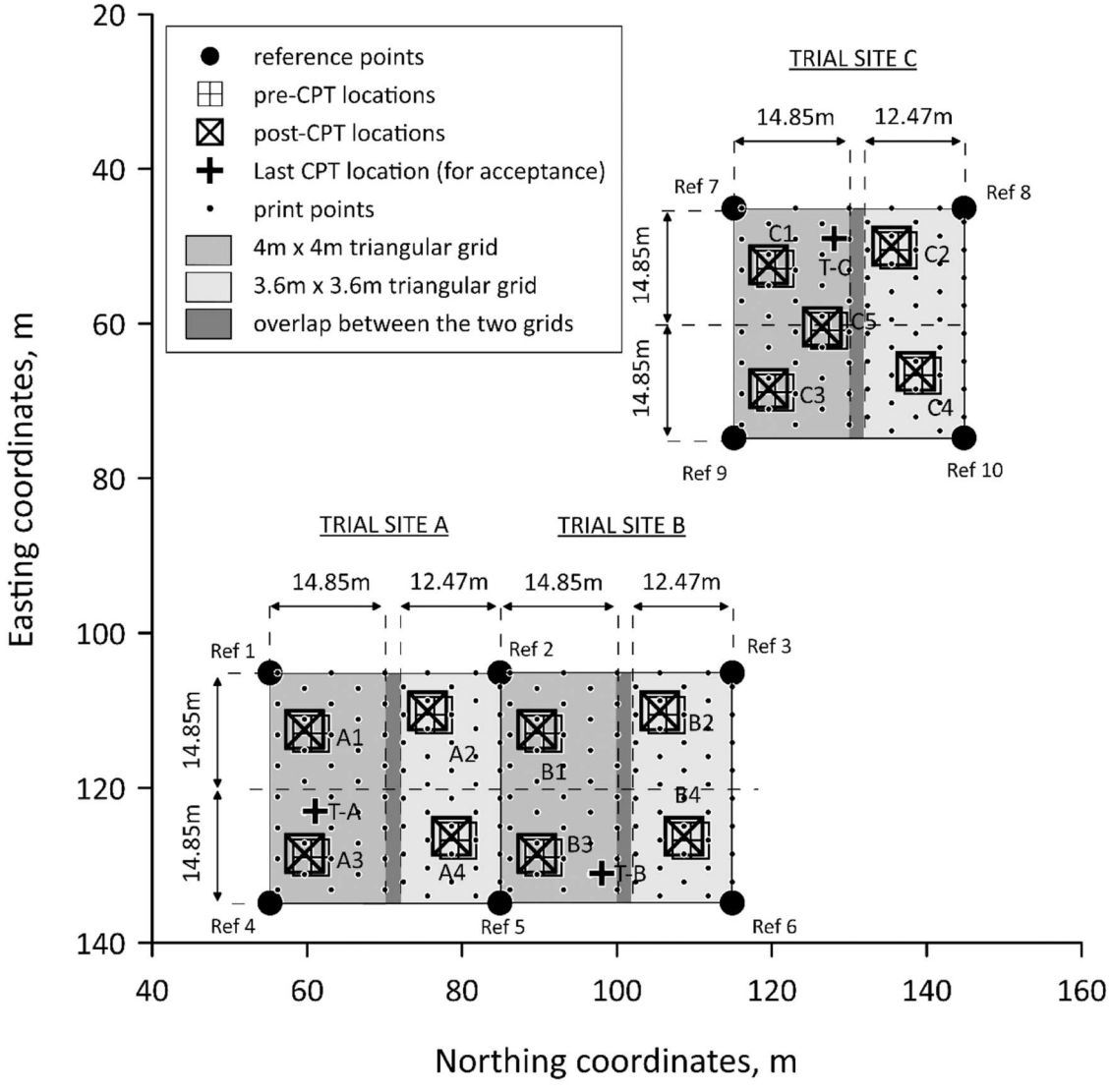

Figure 2. Layout for trial test sites A, B and C.

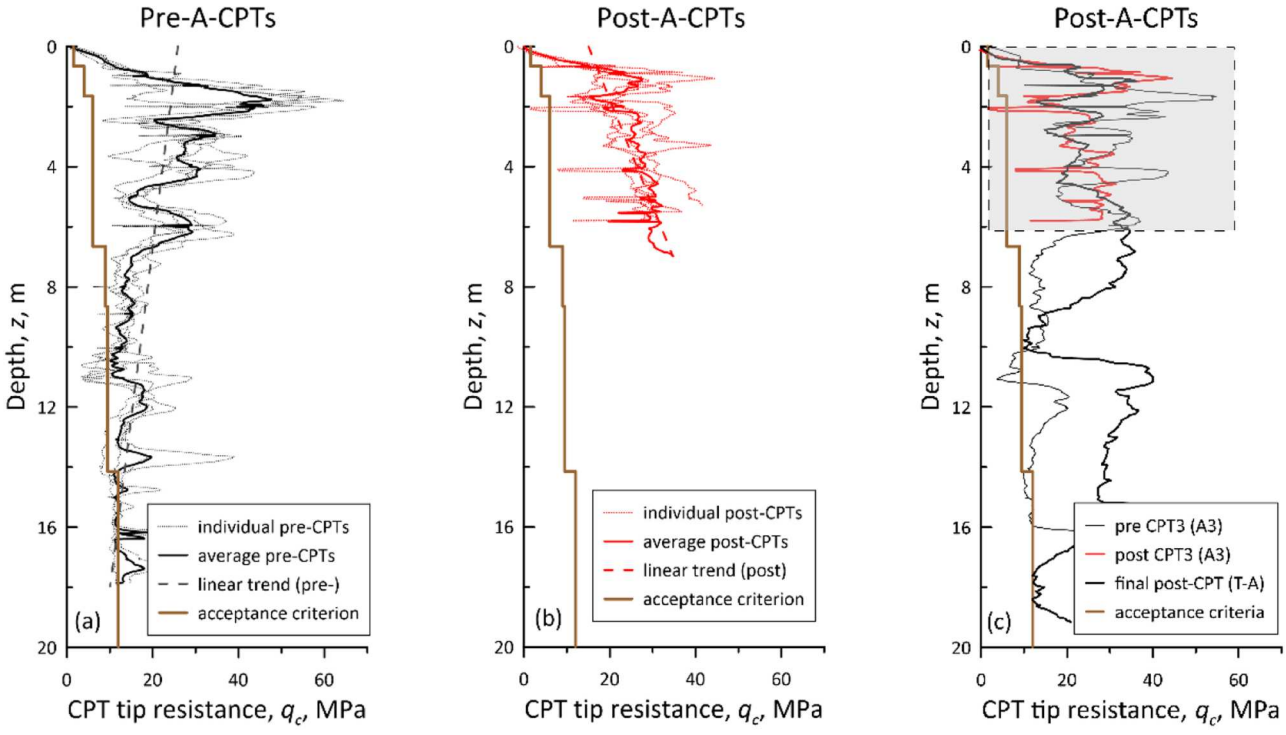

Figure 3. CPT tip resistance measurements from trial test site A: (a) pre-treated; (b) post-treated and (c) acceptance criterion.

larger equilateral triangles (side length of 4 m) also resulted in about 20 prints. All post-CPTs were executed 50 days after the application of ground improvement, ensuring full dissipation of any potential excess pore pressures generated during vibro-compaction.

Figures 3, 5, 7 provide information on the q_c measurements with depth for trial sites A, B and C, respectively. In each figure, Part (a) includes the q_c measurements for each individual pre-CPT, an averaged tip resistance over all pre-CPTs at the test site along with its estimated linear

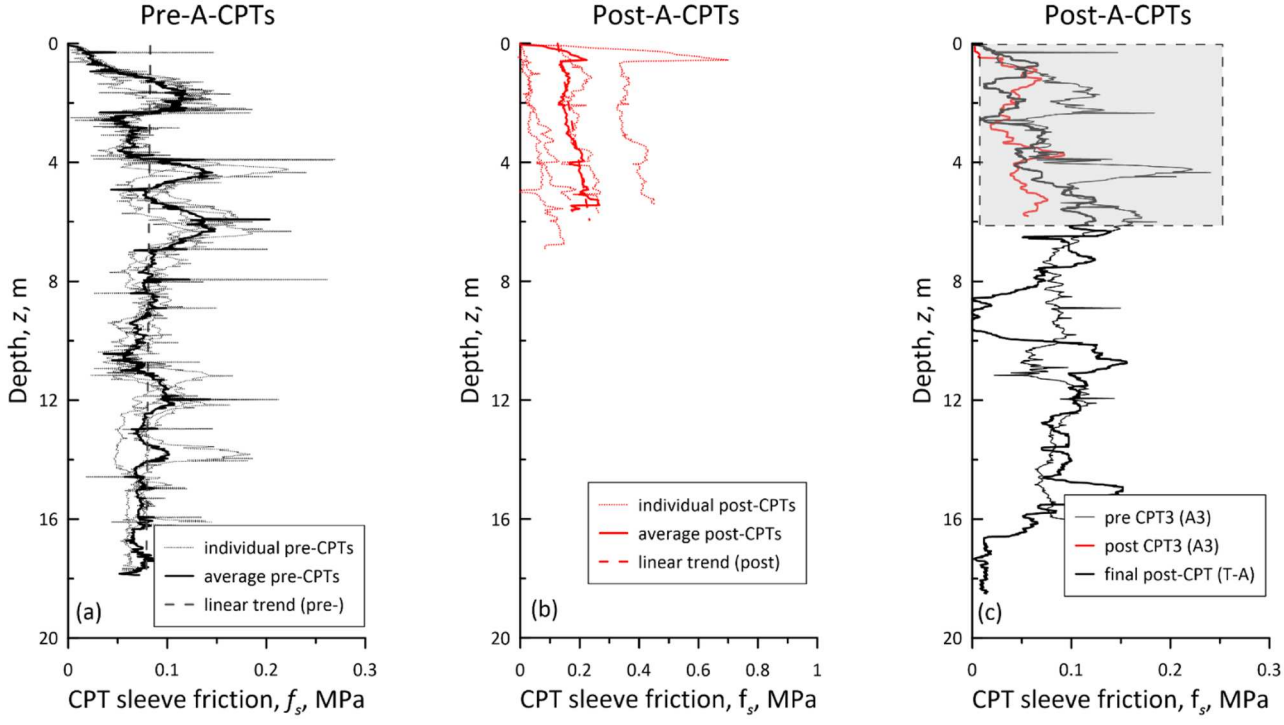

Figure 4. CPT sleeve friction measurements from trial test site A: (a) pre-treated; (b) post-treated and (c) final post CPT.

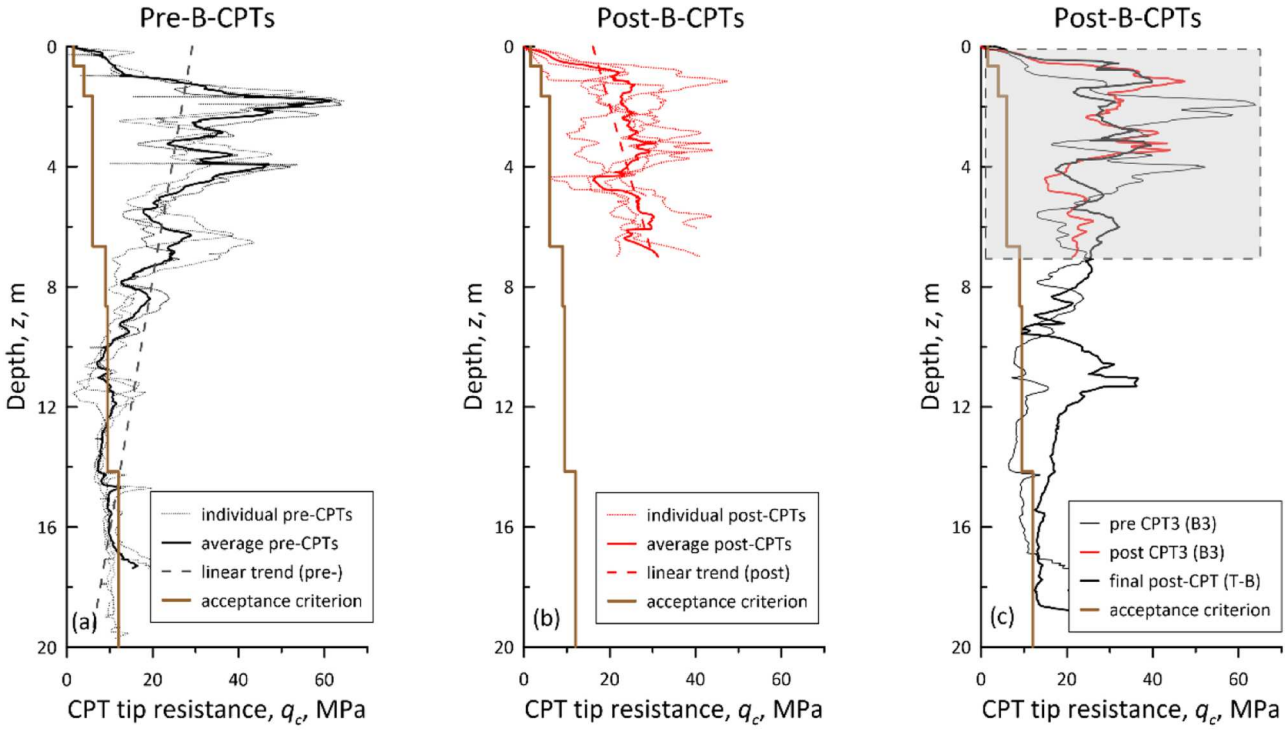

Figure 5. CPT tip resistance measurements from trial test site B: (a) pre-treated; (b) post-treated and (c) acceptance criterion

mean depth-trend (indicated by the dashed line), and the project acceptance criterion for the ground improvement. Part (b) shows equivalent information for the post- CPT tests. Part (c) compares the project acceptance criterion specified by the contractor against the extra, last CPT for the site, and also includes the corresponding closest pre- and post-CPTs for further comparison (see also Figure 2). Equivalent results are presented in Figures 4, 6, 8 for sleeve friction, f_s.

The geostatistical analysis presented next is based on the CPT information presented in Figures 3–8. The data were obtained using a 10 cm^2 tip area cone and a sleeve area of 150 cm^2, with measurements taken every 2 cm. In general, the penetration depths of all pre-CPTs are substantially larger than those for the post-CPTs, with most depths ranging between 15 and 20 m (see Figures 3(a)–8(a)). In contrast, the maximum penetration depth of the post-CPTs is around 7 m (see Figures 3(b)–8(b)). However, the extra CPTs, indicated as T-A, T-B and T-C in Figure 2, have a larger penetration depth of about 20 m (see Figures 3(c)–8(c)) so that the acceptance criterion in the measured tip resistance can be compared for the whole depth (see Figures 3(c), 5(c) and 7(c)). Note that, to facilitate the comparison, the penetration depth considered in the statistical analyses for T-A, T-B and T-C corresponds to the depth of the closest post-CPT as indicated by the shaded area in Figures 3(c)–8(c).

2.1. Point statistics for CPT tip resistance and sleeve friction

To investigate the influence of vibro-compaction on soil heterogeneity and geotechnical uncertainty, it is first useful to statistically characterise the pre- and post-CPT data, including tip resistances q_c and sleeve friction f_s measurements. This is done for each CPT in terms of its point statistics, the mean μ and variance σ^2, and the coefficient of variation (CoV = σ/μ where σ is the standard deviation). For measurements of cone tip resistance, the results of these statistics for trial sites A, B and C are presented in Tables 1–3, respectively. Tables 4–6 show the equivalent results for sleeve friction. Tables 1–6 also include the individual slope m and the intercept b of the estimated linear mean depth-dependent trend t of q_c and f_s for each CPT (i.e. $t = b + mz$).

The effectiveness of the mechanical improvement in the sand state achieved after vibro-compaction can be clearly seen by the overall increased mean tip resistance and mean sleeve friction in each of the post-CPTs when compared against the μ of the corresponding pre-CPTs. This is true for all 3 trial sites, although, as explained next, the percentage increase differs between the sites. The following discussion mostly focusses on the statistics results for tip resistances presented in Tables 1–3 but, in general, similar trends are found for sleeve friction (Tables 4–6).

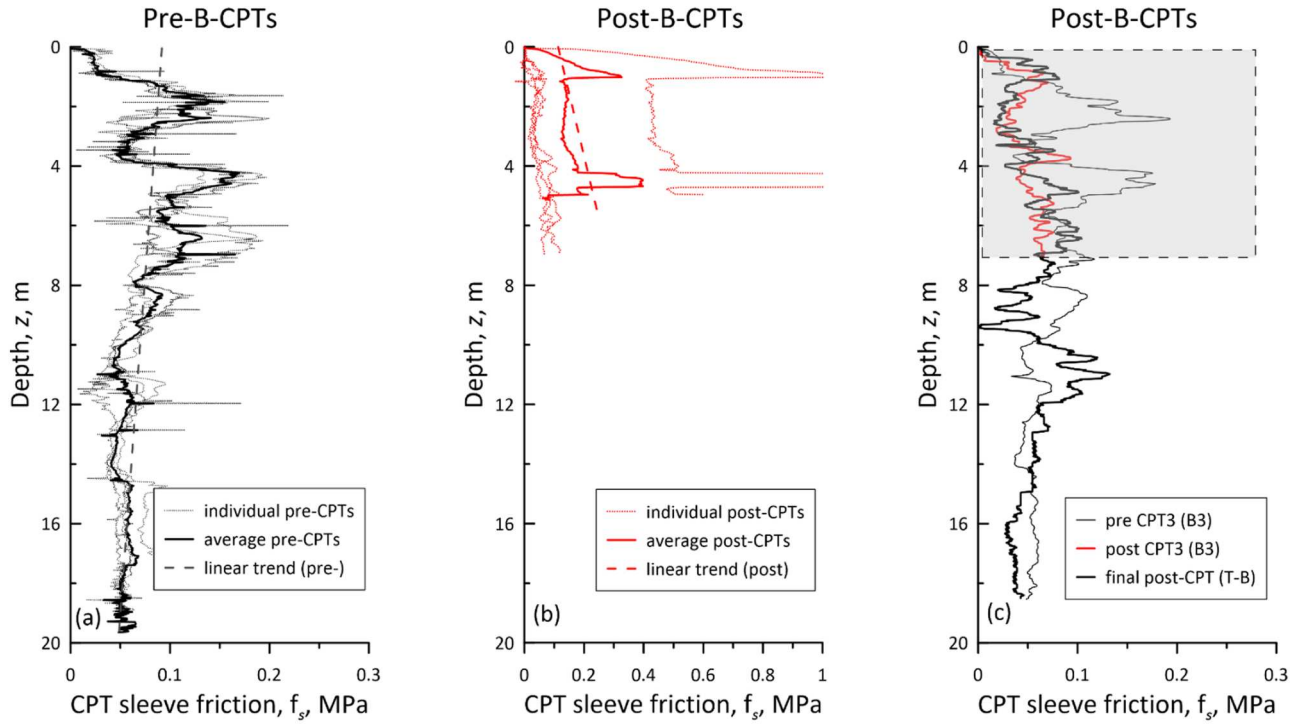

Figure 6. CPT sleeve friction measurements from trial test site B: (a) pre-treated; (b) post-treated and (c) final post CPT.

From the tip resistances before vibro-compaction at trial sites A and B, it is reasonable to infer that the initial state of their sand deposits was relatively looser than at trial site C. Mean values of about 18 MPa are estimated for sites A and B, whereas a value of about 24 MPa is estimated for site C. Similarly, the highest mean value of the sleeve friction corresponds to site C. Given that the effectiveness of vibro-compaction reduces in denser

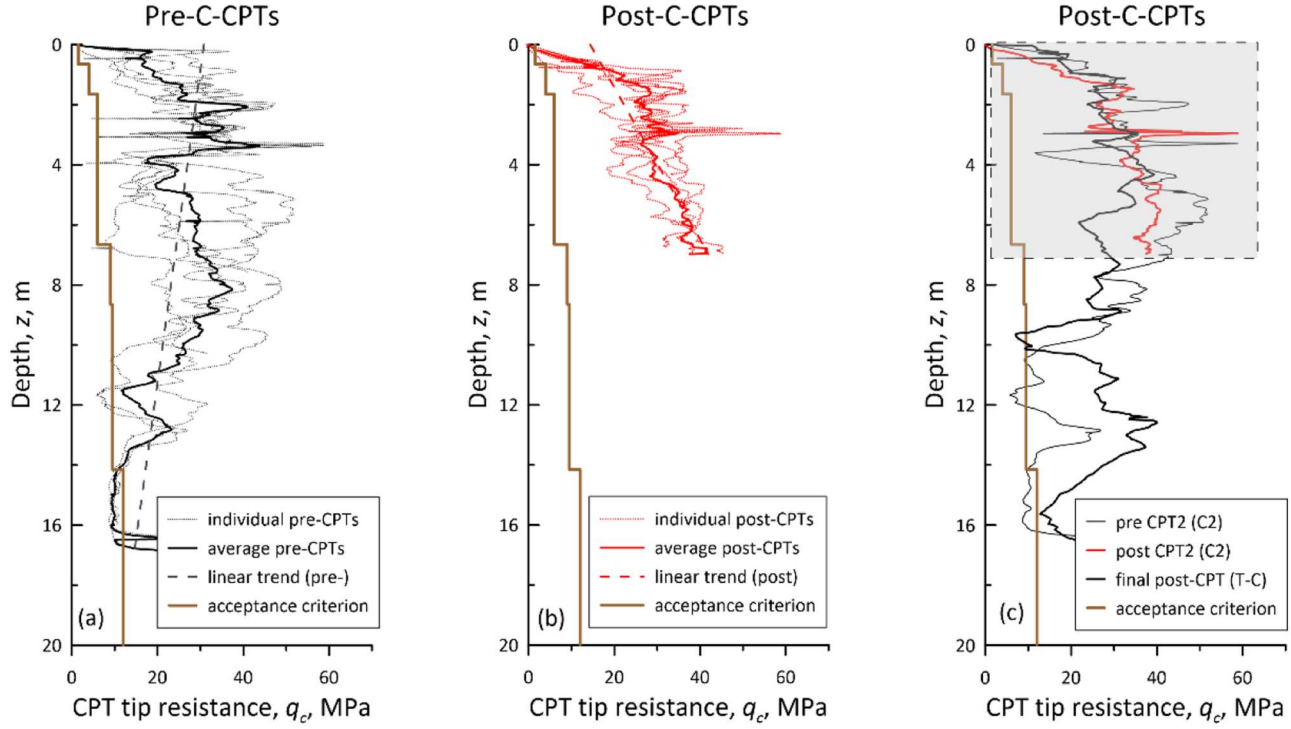

Figure 7. CPT tip resistance measurements from trial test site C: (a) pre-treated; (b) post-treated and (c) acceptance criterion.

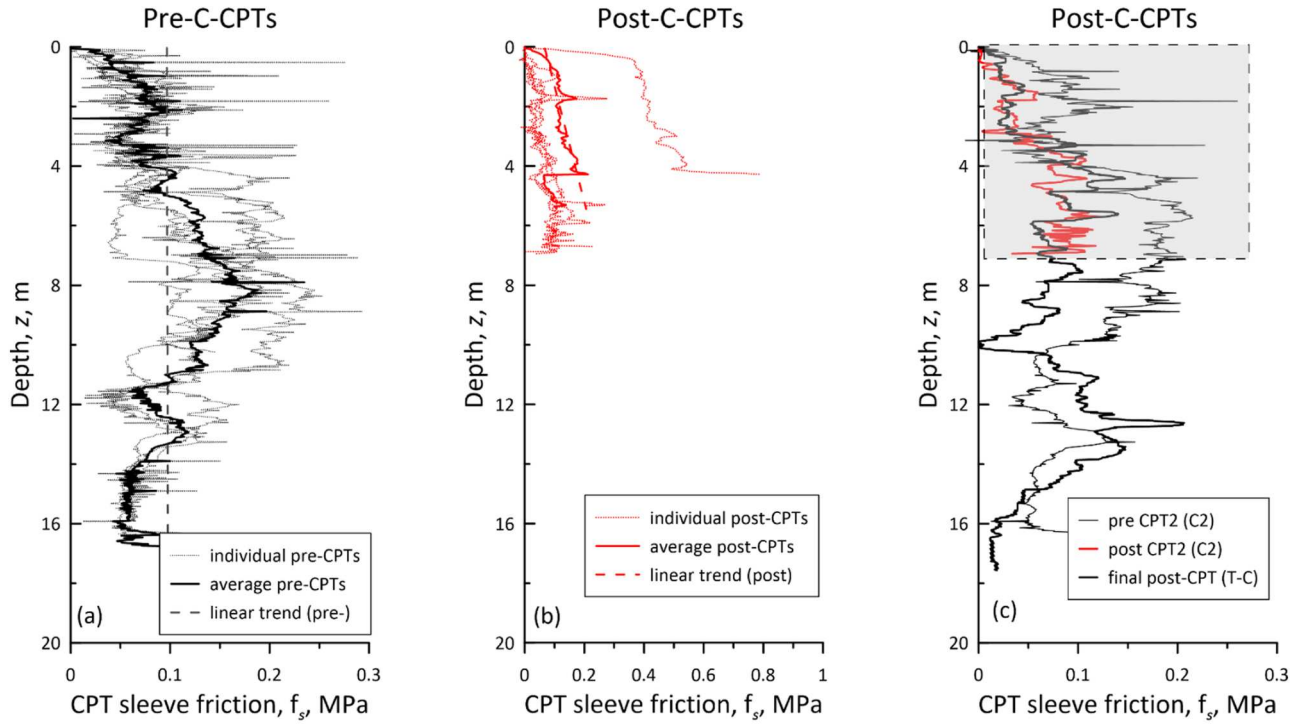

Figure 8. CPT sleeve friction measurements from trial test site C: (a) pre-treated; (b) post-treated and (c) final post CPT.

granular soils (Slocombe, Bell, and Baez 2000), the denser initial state of site C could explain the smaller 10% increase in the averaged mean post q_c (see Table 3), whereas an almost 30% increase is observed at sites A and B (see Tables 1, 2). This explanation also agrees with the smaller 34% increase in the averaged mean post f_s estimated for site C (see Table 6), whereas an over 100% increase is observed at sites A and B (see Tables 4, 5). The higher percentage increase in the averaged f_s compared to the averaged q_c indicates that vibro-compaction causes a significant increase in the in-situ horizontal stress and hence in the coefficient of lateral earth pressure K (where K is defined as the ratio of horizontal to vertical effective stress).

Soil variability in terms of the point variance of tip resistance decreases for all three trial sites after the application of vibro-compaction. This suggests that a more homogenised profile has been achieved, with a reduced dispersion in the tip resistance. The effectiveness of such a reduction seems to improve for more dispersed initial conditions of the sand, as a substantially greater reduction (of over 45%) is observed for trial site B where the initial point variance is largest (143.3 MPa^2). A reduction of about 20–30% is observed for sites A and C, respectively. Interestingly, the level of homogenisation achieved at all sites after the application of vibro-compaction is relatively similar in terms of σ^2, with averaged point variance values ranging between 80 and 90 MPa^2 (as opposed to 100–140 MPa^2 observed in the pre-CPTs), which seems to reflect a consistent execution of the vibro-compaction method. The estimated point variance values of sleeve friction before vibro-compaction are very small and remain small (although, on average, the results show an increasing tendency) after the application of the ground improvement method (Tables 4–6). The averaged increased variance in the post-CPT

Table 1. Tip resistance point statistics for trial test site A.

	Pre-CPT					Post-CPT				
Trial site A	μ: (MPa)	σ^2: (MPa)^2	CoV: (–)	m: (MPa/m)	b: (MPa)	μ: (MPa)	σ^2: (MPa)^2	CoV: (–)	m: (MPa/m)	b: (MPa)
A1	18.30	85.77	0.51	−0.77	24.62	26.13	60.99	0.30	2.39	17.77
A2	17.84	109.91	0.59	−1.05	27.20	22.30	101.56	0.45	6.20	5.74
A3	18.77	107.93	0.55	−1.20	28.56	23.22	79.60	0.38	2.11	16.53
A4	17.92	89.22	0.53	−0.72	24.41	23.99	76.55	0.36	3.60	14.00
T-A	–	–	–	–	–	22.00	63.30	0.36	2.71	14.11
Average	**18.21**	**98.21**	**0.54**	**−0.94**	**26.20**	**23.53**	**76.40**	**0.37**	**3.40**	**13.63**

Note: μ, mean; σ^2, variance; CoV, coefficient of variation; m, slope and b, intercept.

Table 2. Tip resistance point statistics for trial test site B.

	Pre-CPT					Post-CPT				
Trial site B	μ: (MPa)	σ^2: (MPa)^2	CoV: (–)	*m*: (MPa/m)	*b*: (MPa)	μ: (MPa)	σ^2: (MPa)^2	CoV: (–)	*m*: (MPa/m)	*b*: (MPa)
B1	17.47	150.13	0.70	−1.39	30.70	18.06	94.85	0.54	4.23	7.45
B2	16.91	164.34	0.76	−1.41	30.88	19.43	53.43	0.38	2.77	9.74
B3	18.81	145.44	0.64	−1.15	29.51	25.73	84.84	0.36	−0.93	28.97
B4	17.87	113.41	0.60	−1.15	27.89	26.12	96.05	0.38	4.29	13.07
T-B	–	–	–	–	–	24.87	55.04	0.30	−0.90	29.22
Average	**17.77**	**143.33**	**0.67**	**−1.28**	**29.74**	**22.84**	**76.84**	**0.39**	**1.89**	**17.69**

Note: μ, mean; σ^2, variance; CoV, coefficient of variation; *m*, slope and *b*, intercept.

Table 3. Tip resistance point statistics for trial test site C.

	Pre-CPT					Post-CPT				
Trial site C	μ: (MPa)	σ^2: (MPa)^2	CoV: (–)	*m*: (MPa/m)	*b*: (MPa)	μ: (MPa)	σ^2: (MPa)^2	CoV: (–)	*m*: (MPa/m)	*b*: (MPa)
C1	26.36	198.56	0.53	−0.80	32.77	25.81	80.38	0.35	2.58	17.11
C2	25.35	187.49	0.54	−1.62	38.67	31.02	107.27	0.33	4.07	16.77
C3	20.05	60.43	0.39	0.23	18.87	25.62	72.04	0.33	3.98	14.77
C4	22.75	84.67	0.40	1.36	17.59	29.70	98.08	0.33	3.64	17.02
C5	23.76	90.09	0.40	−1.16	33.54	20.07	126.17	0.56	8.94	0.24
T-C	–	–	–	–	–	27.92	39.75	0.23	1.39	23.09
Average	**23.65**	**124.25**	**0.45**	**−0.40**	**28.29**	**26.69**	**87.28**	**0.36**	**4.10**	**14.83**

Note: μ, mean; σ^2, variance; CoV, coefficient of variation; *m*, slope and *b*, intercept.

Table 4. Sleeve friction point statistics for trial test site A.

	Pre-CPT					Post-CPT				
Trial site A	μ: (MPa)	σ^2: (MPa)^2	CoV: (-)	*m*: (MPa/m)	*b*: (MPa)	μ: (MPa)	σ^2: (MPa)^2	CoV: (-)	*m*: (MPa/m)	*b*: (MPa)
A1	0.08	1.1E−03	0.42	7.4E−04	0.07	0.06	1.6E−03	0.72	0.02	−0.01
A2	0.08	1.1E−03	0.43	−8.8E−04	0.09	0.07	1.9E−03	0.64	0.03	0.00
A3	0.09	1.6E−03	0.46	−1.6E−04	0.09	0.21	1.5E−03	0.19	0.02	0.15
A4	0.08	1.1E−03	0.43	8.4E−04	0.07	0.38	6.3E−03	0.21	0.01	0.34
T-A	–	–	–	–	–	0.07	1.7E−03	0.61	5.0E−04	0.06
Average	**0.08**	**1.3E−03**	**0.44**	**1.4E−04**	**0.08**	**0.16**	**2.6E−03**	**0.47**	**0.02**	**0.11**

Note: μ, mean; σ^2, variance; CoV, coefficient of variation; *m*, slope and *b*, intercept.

Table 5. Sleeve friction point statistics for trial test site B.

	Pre-CPT					Post-CPT				
Trial site B	μ: (MPa)	σ^2: (MPa)^2	CoV: (–)	*m*: (MPa/m)	*b*: (MPa)	μ: (MPa)	σ^2: (MPa)^2	CoV: (–)	*m*: (MPa/m)	*b*: (MPa)
B1	0.07	3.5E−03	0.86	−1.9E−03	0.09	0.56	7.8E−02	0.50	0.07	0.39
B2	0.07	1.7E−03	0.62	−2.7E−03	0.09	0.06	9.8E−04	0.52	0.01	0.01
B3	0.07	1.1E−03	0.47	−2.3E−03	0.09	0.05	3.0E−04	0.36	2.5E−03	0.04
B4	0.08	1.0E−03	0.41	−1.1E−03	0.09	0.05	1.2E−03	0.74	0.02	4.2E−03
T-B	–	–	–	–	–	0.06	6.2E−04	0.45	3.0E−05	0.05
Average	**0.07**	**1.8E−03**	**0.59**	**−2.0E−03**	**0.09**	**0.15**	**1.6E−02**	**0.51**	**0.02**	**0.10**

Note: μ, mean; σ^2, variance; CoV, coefficient of variation; *m*, slope and *b*, intercept.

data for f_s seems to suggest, as further discussed later, that the ground improvement in the horizontal direction due to vibro-compaction is less uniform.

The dispersion in the measured values of q_c can be further described by the CoV, for which the average value consistently reduces for all three sites after vibro-compaction. Decreases of about 30–40% are observed for trial sites A and B, respectively, and about 20% for C. The values of the CoVs corresponding to each individual pre-CPT are also quite consistent. For example, at trial site A, the pre- CoV values range from 0.51 to 0.59 (see Table 1), whereas at trial sites B and C the range is 0.60–0.76 (see Table 2) and 0.39–0.53 (see Table 3), respectively. Variations in the individual post- CoVs are marginally larger but still relatively consistent. The only pair of CPTs in which the CoV increases after vibro-compaction corresponds to C5 in Table 3. This behaviour can be explained by the

Table 6. Sleeve friction point statistics for trial test site C.

	Pre-CPT					Post-CPT				
Trial site C	μ: (MPa)	σ^2: $(MPa)^2$	CoV: (-)	m: (MPa/m)	b: (MPa)	μ: (MPa)	σ^2: $(MPa)^2$	CoV: (-)	m: (MPa/m)	b: (MPa)
C1	0.12	5.2E−03	0.62	1.7E−03	0.10	0.06	2.1E−03	0.76	0.02	−1.6E−03
C2	0.10	2.9E−03	0.52	−2.4E−03	0.12	0.06	1.1E−03	0.57	0.01	0.01
C3	0.07	1.2E−03	0.47	7.4E−03	0.04	0.08	2.1E−03	0.61	0.02	0.03
C4	0.07	3.2E−03	0.78	1.2E−02	0.03	0.06	1.2E−03	0.62	0.01	0.01
C5	0.10	1.9E−03	0.43	−7.0E−05	0.10	0.44	6.0E−03	0.18	0.07	0.27
T-C	-	-	-	-	-	0.07	1.7E−03	0.60	8.0E−04	0.06
Average	**0.09**	**2.9E−03**	**0.56**	**3.8E−03**	**0.08**	**0.13**	**2.4E−03**	**0.56**	**0.02**	**0.06**

Note: μ, mean; σ^2, variance; CoV, coefficient of variation; m, slope and b, intercept.

presence of a superficial sand dry crust and shallower interbedded calcarenite layers (as reflected by the very large intercept and negative slope for C5 before vibro-compaction) that is totally or partially broken by the application of vibro-compaction (notice the very small intercept and positive slope of C5 after vibro-compaction). However, the complete removal of these stronger superficial layers depends on the efficacy of the improvement method, which, for this particular case, has not been fully achieved (as reflected by the high variance of the post-CPT C5). In terms of sleeve friction measurements, the estimated CoV values remain approximately the same, which seems to indicate that f_s is less affected than q_c by the application of vibro-compaction (probably because the measurements of f_s already incorporate some spatial averaging).

Tables 1–3 also show the change in sign of the slope of the assumed linear mean depth trend over each individual CPT after applying vibro-compaction (see also Figures 2–4), which is favourable for geotechnical design. This change in the sign of m is consistent with the overall decrease of the intercept b observed in the post-CPT data at all sites. Indeed, the application of vibro-compaction homogenises the top soil profile by weakening the stronger top crust (destruction of calcite structure) and strengthening the weaker sand below, causing a reduction in b. Based on the values of μ, σ^2, CoV, m and b presented in Tables 1–3, there is no clear indication that the denser grid of print points (see the lighter areas indicated in Figure 2) produces a better-quality soil.

Figure 9 plots the tip resistance and sleeve friction data for the pre- and post- CPTs at each trial site in the form of histograms to help visualise the change in μ and σ before and after vibro-compaction. This figure shows that vibro-compaction clearly affects the shape of the histogram, although the exact pattern of this influence is somewhat inconclusive. However, the moderate overall translation of the histogram to higher values of tip resistance and sleeve friction (reflecting higher mean values) is a clear trend observed for all three sites.

The de-trending of q_c and f_s was performed by removing the linear mean depth trend (defined by b and m) for each CPT (see Tables 1–6). The de-trended tip resistances (or sleeve friction measurements) were then divided by the standard deviation of the de-trended data (σ_{res}). This process of de-trending and normalising the CPT tip resistance (or sleeve friction) was carried out in order to approximate the data to a stationary system, which is a requirement for the geostatistical approach used in the next section to estimate the correlation length (Lloret-Cabot, Fenton, and Hicks 2014). In the context of geotechnical engineering, stationarity means that the mean, variance and higher order moments of the soil property being considered are constant in space. Weak stationarity requires that the mean and variance are constant so that the autocorrelation structure depends only on the distance between the observations (i.e. lag τ) and this is the assumption adopted here. As discussed in Jaksa, Kaggwa, and Brooker (1999), it is common practice to transform a non-stationary soil data set to a stationary one by simply removing a low-order polynomial trend. The subsequent normalisation of the de-trended data achieves a constant unit variance. Figure 10 shows the histograms and Gaussian distribution fits to the CPT data after this de-trending and normalising process. The figure demonstrates that the Gaussian distribution provides a good representation of the de-trended and normalised q_c and f_s, especially after the application of vibro-compaction (post-CPTs), which is consistent with the Gaussian field of a random property generated by LAS (Fenton and Vanmarcke 1990). Remarkably similar histograms are observed for all trial sites after the application of vibro-compaction, which suggests a proper execution of vibro-compaction in the project resulting in a more homogenised profile. The point-wise variability in the pre tip resistances (as well as in the pre sleeve friction measurements) is quite consistent between the histograms for the three sites, especially for sites A and B (see Figure 7(a, b)).

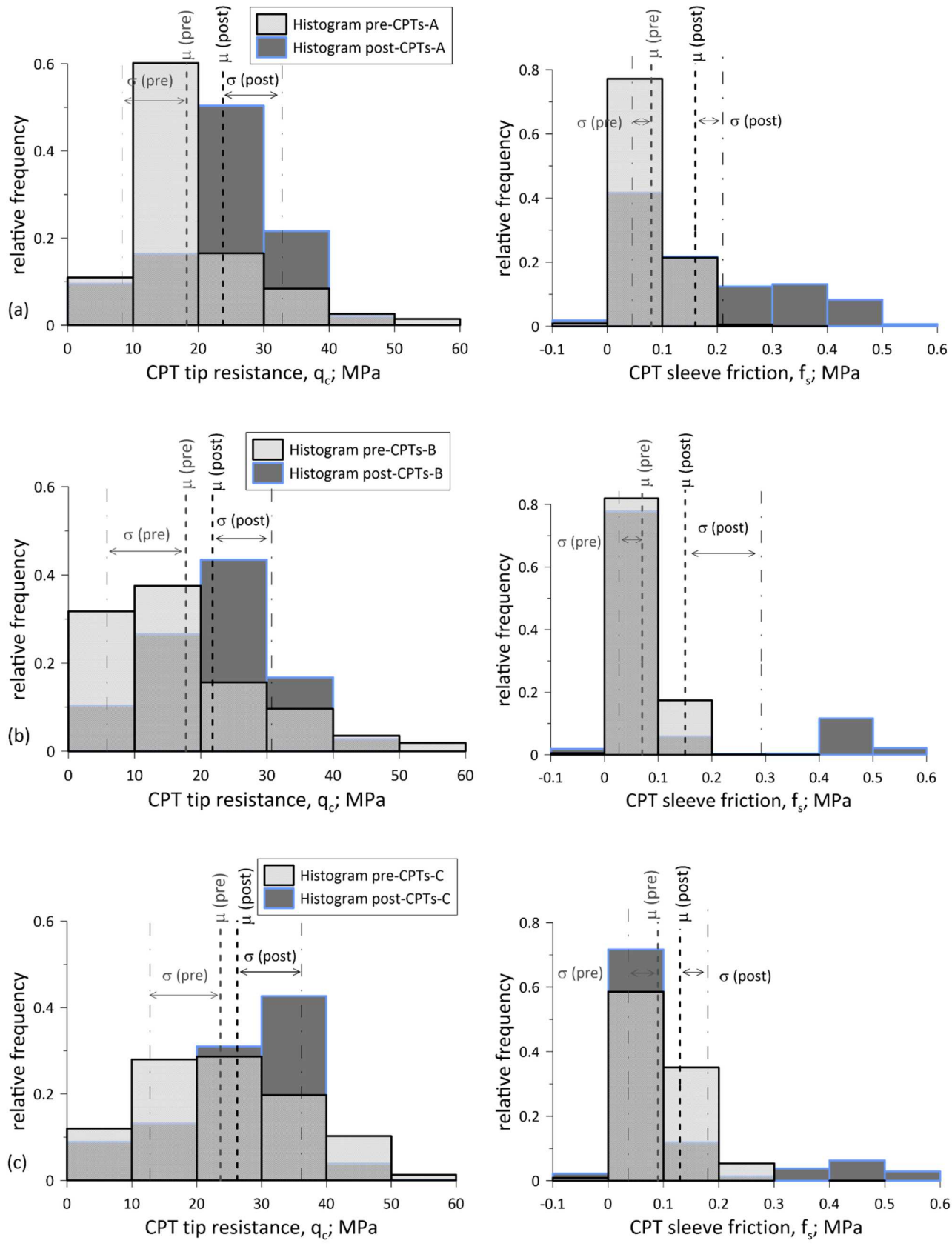

Figure 9. Histograms for pre- and post- CPT data: (a) trial site A; (b) trial site B and (c) trial site C.

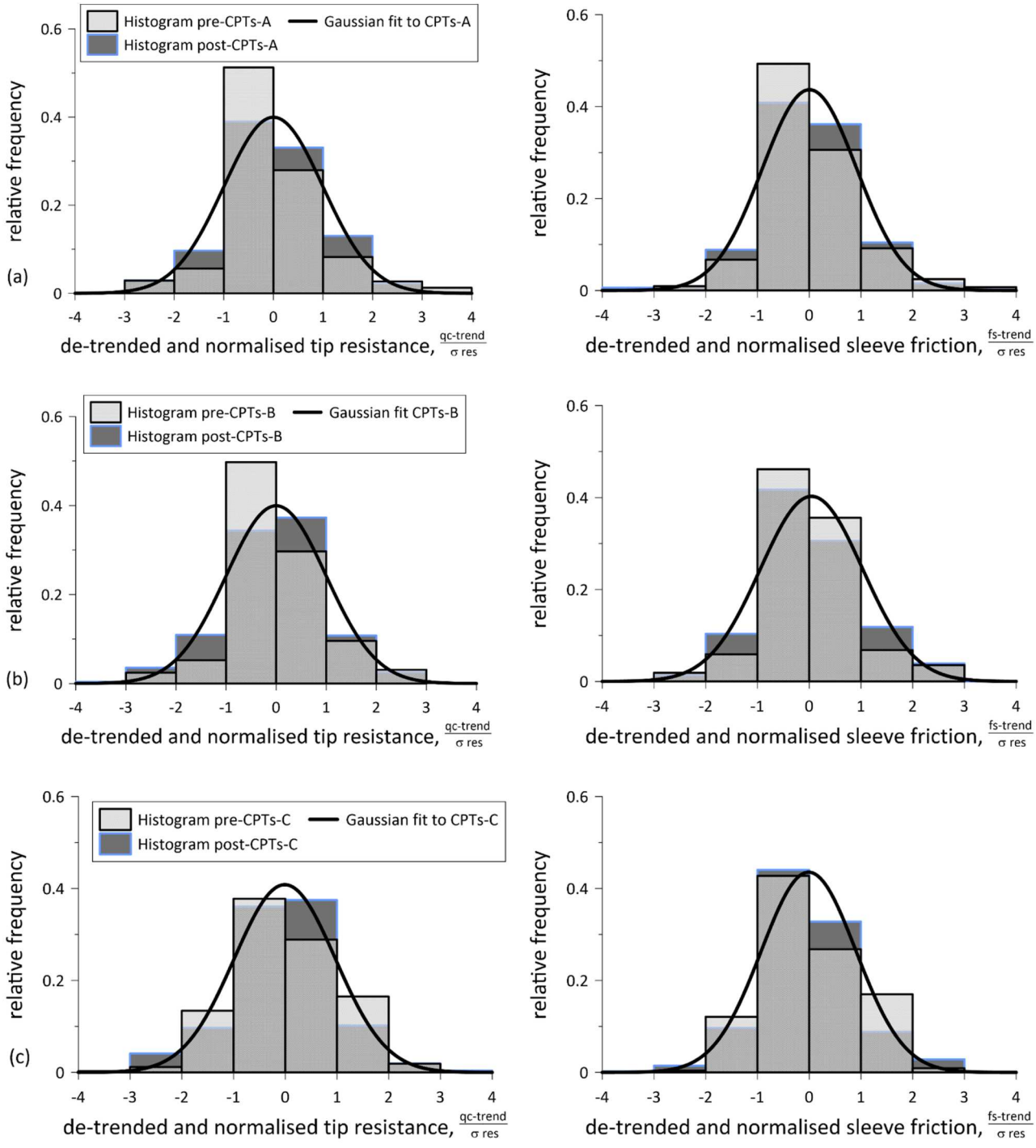

Figure 10. Histograms and probability distribution fits for de-trended and normalised pre- and post- CPT data: (a) trial site A; (b) trial site B and (c) trial site C.

2.2. Spatial statistics for CPT tip resistance and sleeve friction

Capturing the spatial nature of the variation of a soil property is of particular importance. As discussed earlier, a useful spatial statistic for its characterisation in the vertical direction is the vertical correlation length θ_v, which is estimated relatively easily from in-situ CPT data because of the large amount of equi-spaced values available vertically, i.e. measurements every 2 cm. An important requirement to estimate θ is that the data are statistically homogeneous (or stationary), which can be achieved, at least approximately, by de-trending and subsequently normalising the CPT data as discussed previously. There are various methods available for estimating θ_v from CPT data, as discussed,

for instance, in Lloret-Cabot, Fenton, and Hicks (2014) and Cami et al. (2020). A simple approach is to estimate the experimental correlation structure $\hat{\rho}$ (which may also be named here as the auto-correlation function since only q_c or f_s are involved in the calculation) from available CPT data and best fit it with a theoretical correlation function ρ. Although other alternatives are possible, this research assumes a Markovian theoretical correlation (or auto-correlation) function, given by:

$$\rho(\tau) = exp\left\{-\frac{2|\tau|}{\theta}\right\} \quad (1)$$

where τ is the lag distance. The experimental correlation function has been estimated as:

$$\hat{\rho}(j\tau) = \frac{1}{(n-j-1)\hat{\sigma}^2}\sum_{i=1}^{n-j}(X_i - \hat{\mu})(X_{i+j} - \hat{\mu}) \quad (2)$$

where τ is the lag distance in a given direction between sample observations $X_1, X_2, \ldots X_n$, $\hat{\mu}$ is the estimated mean, and $\hat{\sigma}^2$ is the estimated point variance. For correlation in the vertical direction, n is the total number of data points in the CPT profile.

This method has been applied to each CPT. Hence, at trial site A, four values of θ_v are obtained from the four pre-CPTs available and five further values of θ_v are obtained from the five CPTs available after vibro-compaction (i.e. four post-CPTs plus T-A, see Figure 2), and similarly for the other two sites. Furthermore, for each site, a representative mean value of θ_v before vibro-compaction is obtained by averaging the calculated individual values of θ_v from each pre-CPT, and similarly for after vibro-compaction. The results from these calculations are presented later in tabular form for the 3 sites.

A second approach to estimating a representative mean value of θ_v before and after vibro-compaction has also been considered, and this gives comparable results to analysing the individual θ_vs. This is based on obtaining an average vertical experimental correlation function from the individual vertical experimental correlation functions (Equation 2), and then best fitting this function to the theoretical correlation function (Equation 1) to obtain a single value of θ_v. The results corresponding to tip resistances for sites A, B and C are illustrated in Figures 11–13, respectively, with Parts (a) and (b) of the figures showing, respectively, the information before and after vibro-compaction. Figures 14–16 show equivalent results for sleeve friction.

The estimation of the horizontal correlation length θ_h is more challenging, because less data are available in the horizontal direction and these data are commonly not equi-spaced (although the latter is not necessarily a disadvantage for the estimation of θ_h, as discussed in Ching et al. (2018)). The typical scarcity of data in the horizontal direction means that some assumptions are often needed to estimate θ_h and less reliable estimates are typically obtained. In this context, the main assumption needed in this research is that an equivalent correlation structure is assumed in any direction within a given horizontal plane and that this hypothesis holds for each depth (thus, over the whole CPT depth at

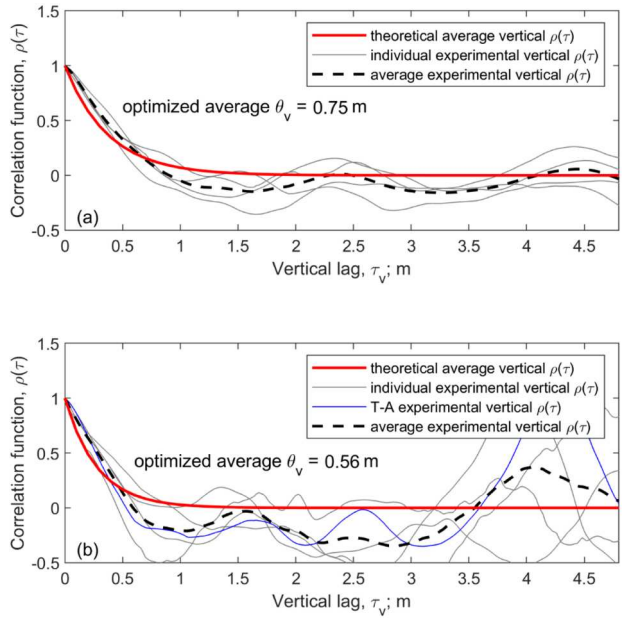

Figure 11. Estimation of the q_c vertical correlation length for trial test site A: (a) before and (b) after vibro-compaction.

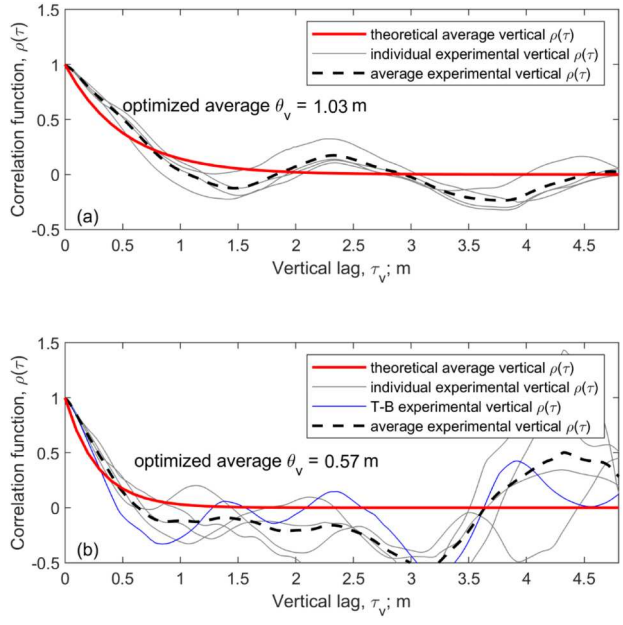

Figure 12. Estimation of the q_c vertical correlation length for trial test site B: (a) before and (b) after vibro-compaction.

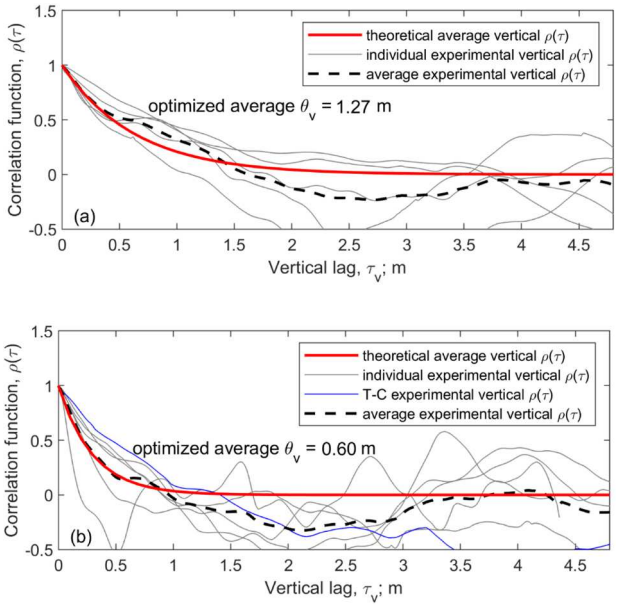

Figure 13. Estimation of the q_c vertical correlation length for trial test site C: (a) before and (b) after vibro-compaction.

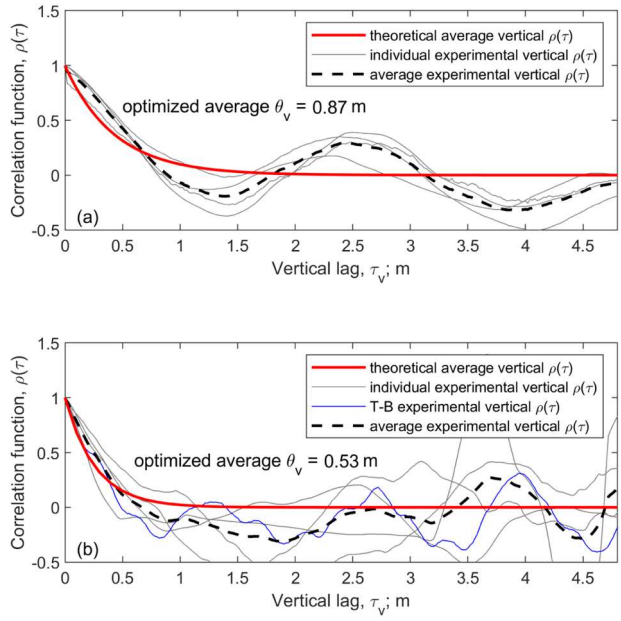

Figure 15. Estimation of the f_s vertical correlation length for trial test site B: (a) before and (b) after vibro-compaction.

each 0.02 m interval). Another important assumption is that all profiles are off-set to a common zero-depth, so that the ground surface is at the same level for each site. These are reasonable assumptions here, given the sedimentary nature and relatively flat surface of the ground investigated, plus the fact that all three trial sites are relatively close to each other (see Figure 2). Under these assumptions, it is possible to estimate the experimental correlation function at various specific horizontal lags, considering that the horizontal distance between any two CPTs (before or after vibro-compaction) corresponds to a particular horizontal lag. For example, in addition to $\tau_{h0} = 0$ m, three further horizontal lags can be considered between the four pre-CPTs available at trial site A (see Figure 2). Three pre-CPT pairs are separated by a distance of about $\tau_{h1} = 16.5$ m (A1-A2, A1-A3 and A2-A4). One pair of pre-CPTs is separated by a distance of $\tau_{h2} = 19$ m (A3-A4) and two pairs by $\tau_{h3} \approx 24$ m (A1-A4 and A2-A3).

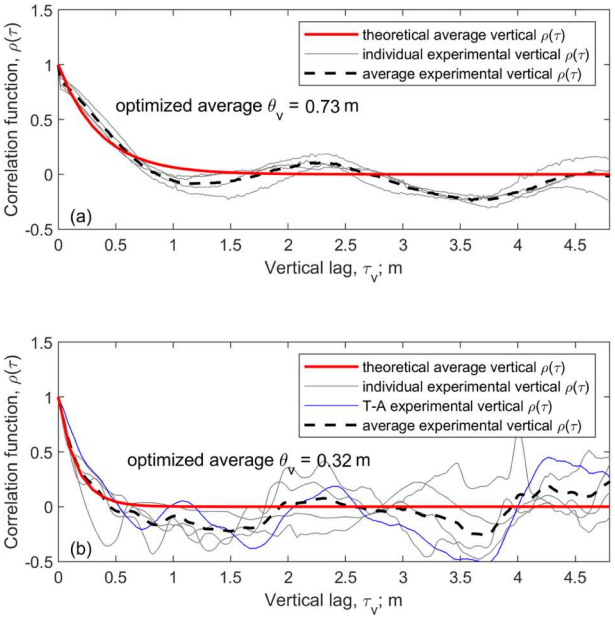

Figure 14. Estimation of the f_s vertical correlation length for trial test site A: (a) before and (b) after vibro-compaction.

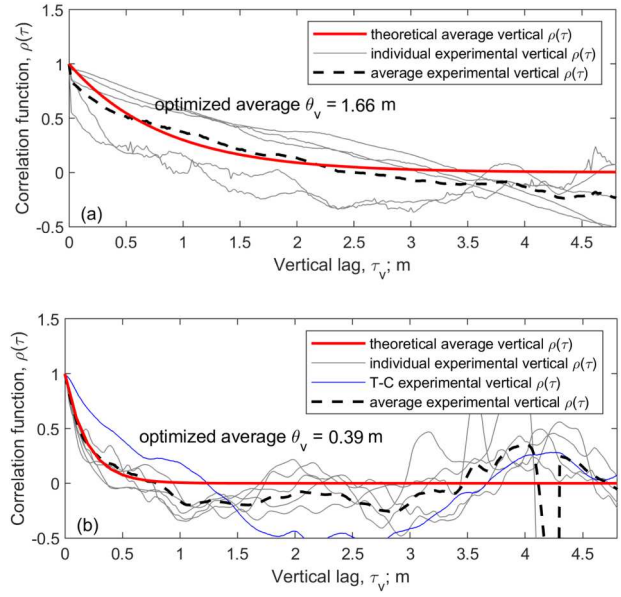

Figure 16. Estimation of the f_s vertical correlation length for trial test site C: (a) before and (b) after vibro-compaction.

As shown later, some additional experimental data are available after vibro-compaction thanks to the extra CPTs T-A, T-B and T-C indicated in Figure 2.

At each measurement level of a given pair of CPTs separated by one of these lags, a value of the experimental horizontal correlation structure can be found by applying Equation 2 in the horizontal direction, with $\hat{\mu}$ and $\hat{\sigma}$ being the mean and the standard deviation of all CPT data involved in the calculation (i.e. over the depth range considered). Importantly, when using Equation 2 to calculate $\hat{\rho}(\tau)$ in the horizontal direction, the two CPTs need to be analysed over exactly the same depth range. Hence, if their respective penetration depths are slightly different, the smaller penetration depth is taken to be the limiting depth. For a given τ_h, the final estimated $\hat{\rho}(\tau_h)$ is the average of all individual $\hat{\rho}$s over the depth range considered. Note that, when more than one pair of data is available for a particular τ_h (as, for instance, in the case of $\tau_h = 16.5$ m discussed above), the overall averaged $\hat{\rho}$ between all pairs is taken.

Given that applying this process to the pre-CPT data from trial sites A and B results in only three relevant values of $\hat{\rho}$ (i.e. corresponding to $\tau_h = 16.5$, 19 and 24 m), and considering the fact that sites A and B are next to each other (see Figure 2), a further two horizontal lags are considered only for the analysis of the horizontal correlation structure before vibro-compaction at these trial sites. These two additional horizontal lags correspond to the closest pairs of pre-CPTs between the two sites and hence have the shorter lag distances

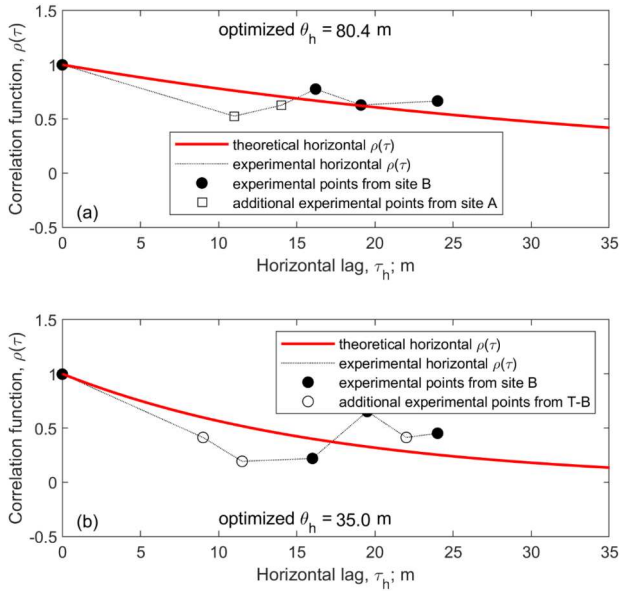

Figure 18. Estimation of the q_c horizontal correlation length for trial test site B: (a) before and (b) after vibro-compaction.

(i.e. $\tau_{h4} = 11$ m for A4-B3 and $\tau_{h5} = 14$ m for A2-B1, see Figure 2). Values of the experimental correlation structure at short lags (relative to the estimated θ_h) are especially useful in estimating θ_h, because, as highlighted in DeGroot and Baecher (1993), they play a more important role in the best fitting strategy than experimental correlation structure values at large lags. Further details on the estimation of the horizontal correlation length can be found elsewhere (Ching et al.

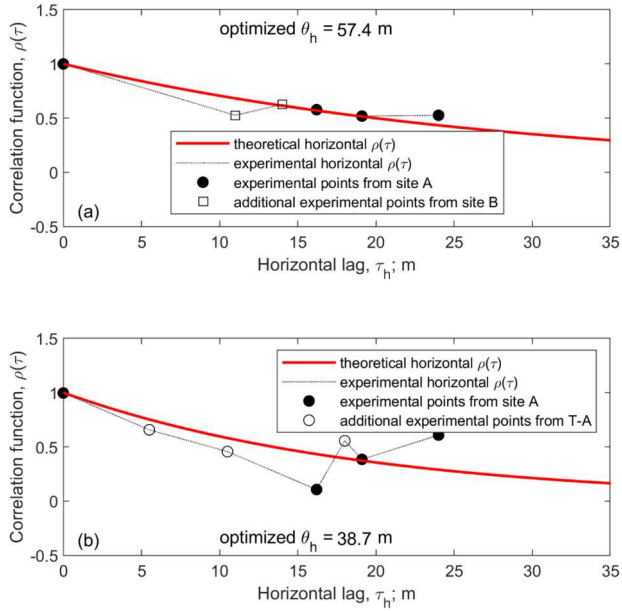

Figure 17. Estimation of the q_c horizontal correlation length for trial test site A: (a) before and (b) after vibro-compaction.

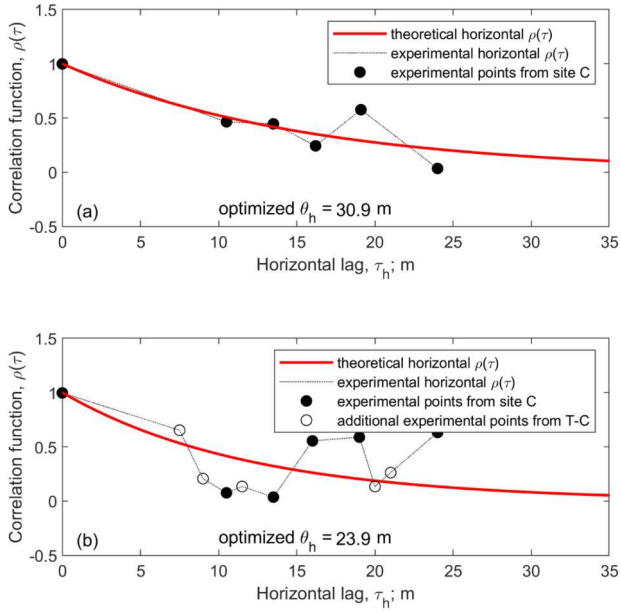

Figure 19. Estimation of the q_c horizontal correlation length for trial test site C: (a) before and (b) after vibro-compaction.

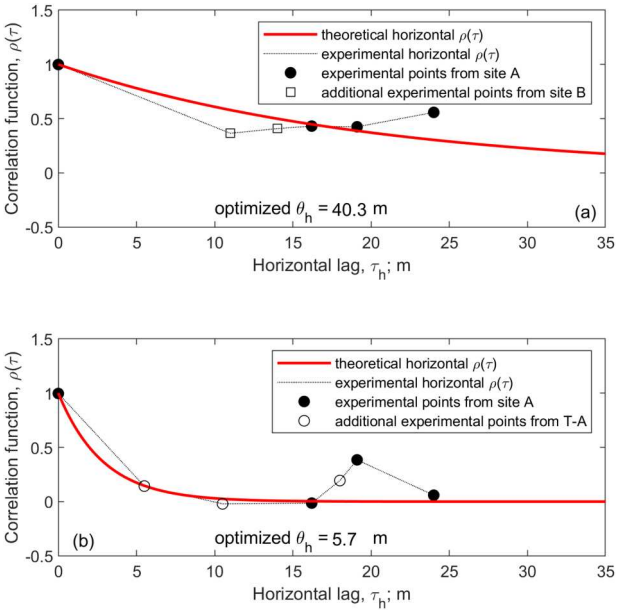

Figure 20. Estimation of the f_s horizontal correlation length for trial test site A: (a) before and (b) after vibro-compaction.

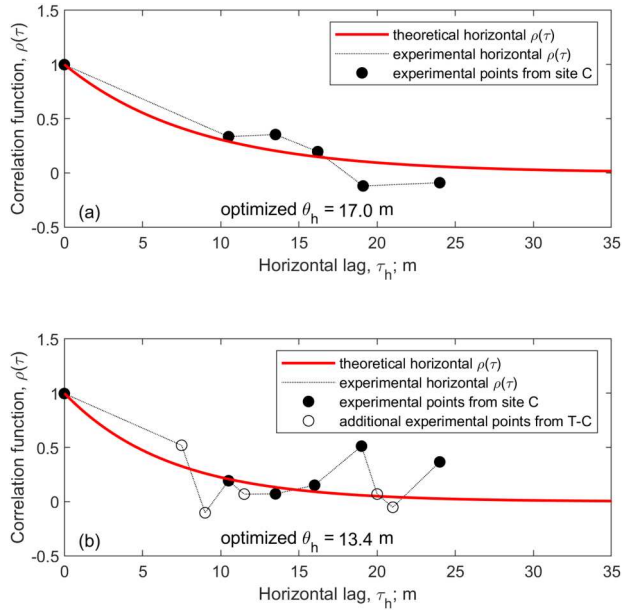

Figure 22. Estimation of the f_s horizontal correlation length for trial test site C: (a) before and (b) after vibro-compaction.

2018; de Gast et al. 2021; Jaksa, Kaggwa, and Brooker 1999; Larsson, Stille, and Olsson 2005; Lloret-Cabot, Fenton, and Hicks 2014).

The results of estimating the horizontal correlation length for q_c are illustrated in Figures 17–19 for trial sites A, B and C, respectively, with Parts (a) and (b) of the figures showing, respectively, the information before and after vibro-compaction. Equivalent information for f_s is given in Figures 20–22. In all these figures, filled symbols indicate values of $\hat{\rho}$ at lags corresponding to pairs of pre- or post-CPTs from the same site being investigated. Figures 17(a) and 18(a) (and, equivalently, Figures 20(a) and 21(a) for f_s) include two additional empty square symbols indicating the extra pair of values of $\hat{\rho}$ corresponding to the adjacent pre-CPTs between trial sites A and B. Meanwhile, the empty circular symbols in Parts (b) of these figures indicate additional values of $\hat{\rho}$ resulting from the extra post-CPT used to assess the project acceptance criterion (T-A, T-B and T-C). A summary of the estimated values of θ_v and θ_h for q_c is given in Tables 7–9 for trial sites A, B and C, respectively. Equivalent information for f_s is provided in the Appendix for completeness (see Tables A1, A2 and A3).

Unlike similar studies on the effects of vibro-compaction in other regions (Cai et al. 2017; Zhai et al. 2024), the estimated θ_v for the tip resistances from the pre-CPTs used in our study is significantly larger than that estimated from the post-CPTs, for all CPTs at all three

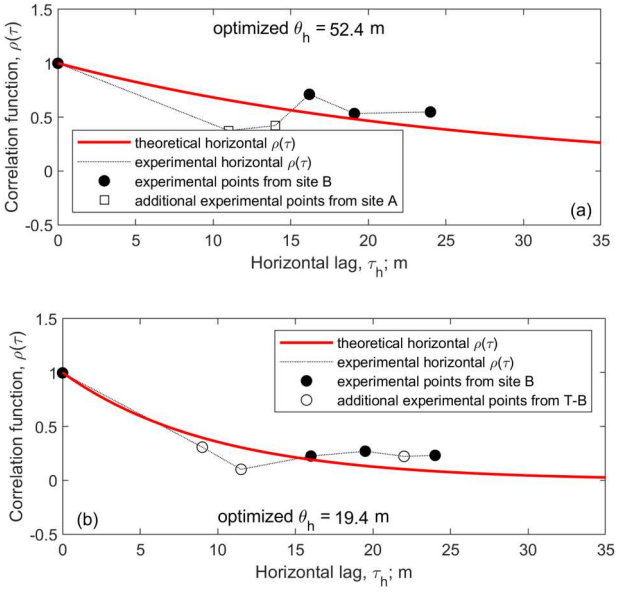

Figure 21. Estimation of the f_s horizontal correlation length for trial test site B: (a) before and (b) after vibro-compaction.

Table 7. Vertical and horizontal correlation lengths for tip resistance at trial test site A.

	Pre-CPT		Post-CPT	
Trial site A	θ_v: (m)	θ_h: (m)	θ_v: (m)	θ_h: (m)
A1	0.80	–	0.68	–
A2	0.60	–	0.54	–
A3	0.78	–	0.36	–
A4	0.89	–	0.71	–
T-A	–	–	0.48	–
Average	**0.77**	**57.4**	**0.55**	**38.7**
σ^2	**0.01**	-	**0.02**	-
CoV	**0.14**	-	**0.23**	-

Note: μ, mean; σ^2, variance; CoV, coefficient of variation and θ, correlation length.

Table 8. Vertical and horizontal correlation lengths for tip resistance at trial test site B.

	Pre-CPT		Post-CPT	
Trial site B	θ_v: (m)	θ_h: (m)	θ_v: (m)	θ_h: (m)
B1	0.99	–	0.69	–
B2	1.31	–	0.60	–
B3	1.16	–	0.55	–
B4	0.80	–	0.60	–
T-B	–	–	0.42	–
Average	**1.07**	**80.4**	**0.57**	**35.0**
σ^2	**0.04**	–	**0.01**	–
CoV	**0.18**	–	**0.09**	–

Note: μ, mean; σ^2, variance; CoV, coefficient of variation and θ, correlation length.

Table 9. Vertical and horizontal correlation lengths for tip resistance at trial test site C.

	Pre-CPT		Post-CPT	
Trial site C	θ_v: (m)	θ_h: (m)	θ_v: (m)	θ_h: (m)
C1	2.06	–	0.70	–
C2	1.84	–	0.74	–
C3	1.13	–	0.43	–
C4	0.76	–	0.71	–
C5	1.29	–	0.17	–
T-C	–	–	0.95	–
Average	**1.42**	**30.9**	**0.62**	**23.9**
σ^2	**0.22**	–	**0.06**	–
CoV	**0.33**	–	**0.41**	–

Note: μ, mean; σ^2, variance; CoV, coefficient of variation and θ, correlation length.

sites, with mean reductions ranging from about 30% for trial site A to about 60% for trial site C (see Tables 7–9, respectively). Even greater differences are observed in terms of f_s, reaching mean reductions of about 70% for trial site C (see Appendix). The variances of the estimated θ_v for q_c are relatively small, ranging from 0.01 to 0.22 for the pre-CPTs and only 0.01 to 0.06 for the post-CPTs. Slightly larger variances of the estimated θ_v are observed in terms of f_s, but still within a similar range. Considering the averaged pre- and post- values for θ_v from all three sites, the application of vibro-compaction reduces the mean estimated θ_v from about 1 m to about 0.5 m, and this reduction holds true for the calculations corresponding to sleeve friction measurements. A possible explanation for such a reduction is given as follows. The mixing of sand caused by vibro-compaction results in a denser and stronger particle arrangement as demonstrated by the overall increased mean tip resistance (and also confirmed by an increased mean sleeve friction). This denser configuration has involved the mixing of sand grains from different depths, with the sand at each depth expected to have had a specific geological history and hence similar geotechnical properties. It is likely that the application of vibro-compaction removes (at least partially) some of the original spatial similarity of soil properties, which could explain the significantly smaller estimated values of vertical correlation length after vibro-compaction.

The application of vibro-compaction also tends to reduce the estimated θ_h, with larger (relative) reductions found in terms of f_s. In terms of q_c, the averaged value of θ_h for all the sites is about 60 m before vibro-compaction and 30 m after, which is consistent with the average reduction observed for θ_v, albeit one order of magnitude higher. In terms of f_s, the averaged value of θ_h for all the sites is about 40 m before vibro-compaction and 15 m after. While tip resistance is primarily influenced by the relative density of sandy soils, sleeve friction is affected by both the relative density and the lateral earth pressure coefficient. The more pronounced reduction in correlation length observed in sleeve friction data is attributed to the vibro-compaction treatment, which not only uniformly densifies the soil but also removes (though not uniformly) the influence of sedimentation history on soil particle orientation, thereby altering the lateral earth pressure coefficient.

It is interesting to see how close the experimental horizontal correlation structure for the q_c of the pre-CPTs is to the horizontal theoretical correlation structure for the largest lags at trial sites A and B (filled symbols in Figures 17(a) and 18(a)). As mentioned previously, these three experimental points at larger lags are calculated using CPTs from the given site, whereas the two additional experimental points at shorter lags (indicated as empty square symbols) involve CPTs from the adjacent site. A reasonable level of correspondence is still seen in these experimental values at shorter lags, which provides confidence on the estimated values for θ_h despite the small number of points available. A similar level of correspondence is observed at trial site C for the experimental points at shorter horizontal lags before application of vibro-compaction, although a relatively larger departure is observed for larger lags (Figure 19(a)). Further inspection of Figures 17(a), 18(a) and 19(a) shows that relatively high correlations are observed for short horizontal lags (up to about $\tau_h = 15$–20 m), with values larger (or slightly less) than 0.5 at all three sites.

The influence of vibro-compaction is clearly seen when comparing the initial high correlations at short lags in the pre-CPT data with the corresponding experimental correlations at similar lags from the q_c of the post-CPT data (Figures 17(b), 18(b) and 19(b)). At all three sites, vibro-compaction alters the original level of soil uniformity achieved during its formation by horizontal deposition, as reflected by the decrease in the experimental correlation at shorter lags (up to about $\tau_h = 15$–20 m, the observed correlation is now lower than 0.5 in most cases). In other words, the mixing of soil due to

vibro-compaction diminishes the layering present in the original soil profile. As expected, the intensity of this effect seems to have a greater influence at shorter lags, which suggests a limiting influence (in terms of τ_h) of the effect of vibro-compaction in the horizontal direction. This observation seems reasonable because, as explained earlier, the efficiency of the mixing reduces with increasing radius from the vibrator. Indeed, large correlations of about 0.5 are still observed for $\tau_h > 20$ m after application of vibro-compaction at all three sites (see Figures 17(b), 18(b) and 19(b)), implying that some of the pre-existing horizontal correlations at larger lags are preserved after the application of vibro-compaction. Similarly, the reduction in the estimated horizontal correlation length of f_s after the application of vibro-compaction can also be explained by the effect of mixing of soil during vibro-compaction, which diminishes the original soil layering, hence reducing θ_h (see Figures 18–20).

3. Conclusions

The influence of vibro-compaction on the heterogeneity of natural sand deposits in Saudi Arabia has been investigated using CPT data before (pre-) and after (post-) application of ground improvement by vibro-compaction. Cone tip resistances and sleeve friction measurements have been statistically interpreted by estimating the mean, variance, coefficient of variation, fitted normal distribution and correlation lengths. In terms of point statistics, the results showed that the application of vibro-compaction consistently increases the mean tip resistance and the mean sleeve friction but, as expected, the size of the increase depends greatly on the initial state of the sand. For instance, in terms of q_c, the initial looser condition of the sand deposits at sites A and B led to a 30% increase in the average tip resistance mean, whereas only 10% was observed for the initially denser sand at trial site C. In contrast, vibro-compaction reduces the dispersion of tip resistance values in terms of point variance and coefficient of variation for all three sites (a less conclusive pattern is observed for f_s, where very small values of point variance are estimated before and after vibro-compaction). Similar to the increased mean, achieving a smaller point variance is advantageous for geotechnical design purposes, as it reduces some of the initial geotechnical uncertainty associated with the heterogeneity of the soil property and, more importantly, a higher representative/characteristic value can be taken (and this is especially true for q_c which directly relates to the undrained shear strength). On average, the percentage reduction in point variance for q_c is as large as 45% for site B, while 20–30% reduction is observed for sites A and C. In terms of CoV, the averaged values estimated from the q_c of the pre-CPTs for all sites range from 0.45 to 0.67, whereas a much narrower range of values is obtained from the averaged CoV of the post-CPTs (0.36–0.39). Once de-trended and normalised, both pre- and post-tip resistances are reasonably well represented by a Gaussian probability density function, and this is confirmed by the results for sleeve friction.

In terms of spatial statistics, vibro-compaction decreased the vertical and horizontal correlation lengths by approximately 50% for q_c and 50–60% for f_s. The average vertical correlation length over all the pre- and post-CPTs available is about 1 and 0.5 m, respectively, for both tip resistance and sleeve friction measurements. In contrast, the averaged value of the horizontal correlation length before and after vibro-compaction for q_c is about 60 and 30 m, respectively, whereas 40 and 15 m are obtained, respectively, for f_s. These differences in the estimated θ show that, in addition to the soil type and ground conditions (i.e. before/after vibro-compaction), the specific correlation length might differ between ground properties. The reduction in θ_h observed after vibro-compaction can be advantageous for geotechnical design, because it increases the amount of averaging along any potential sliding plane and thereby reduces the uncertainty. However, the influence of θ on structural performance and uncertainty is also dependent on the structure dimensions and type of failure mechanism. The effect of vibro-compaction is clearly apparent in the estimated experimental correlation structure, especially for short horizontal lags where a clear reduction of the experimental correlation is observed. In contrast, the effect of vibro-compaction is less apparent at larger horizontal lags, which seems to suggest that some of the geological features present in the sand from their formation are not completely removed by the mixing of the soil grains during application of this ground improvement method.

Acknowledgement

The second author gratefully acknowledges the support provided by the Chinese Scholarship Council (CSC) programme and Durham University, UK. The fourth author is grateful to the British organisation Cara (Council for At-Risk Academics), for providing financial support to undertake part of this study at Durham University, UK.

Disclosure statement

No potential conflict of interest was reported by the author(s).

Funding

This work was supported by Cara; China Scholarship Council.

References

Alonso, E. E., and R. J. Krizek. 1975. "Stochastic Formulation of Soil Properties." In *Proceedings, International Conference on Application of Statistics and Probabilities in Soil and Structural Engineering*, Aachen, Vol. 2, 9–32.

Baecher, G. B., and J. T. Christian. 2005. *Reliability and Statistics in Geotechnical Engineering*. Chichester: John Wiley & Sons.

Baumann, V., and G. E. Bauer. 1975. "The Performance of Foundations on Various Soils Stabilized by the Vibro-Compaction Method." *Canadian Geotechnical Journal* 11 (4): 509–530. https://doi.org/10.1139/t74-056

Cafaro, F., and C. Cherubini. 2002. "Large Sample Spacing in Evaluation of Vertical Strength Variability of Clayey Soil." *Journal of Geotechnical and Geoenvironmental Engineering* 128 (7): 558–68. https://doi.org/10.1061/(ASCE)1090-0241(2002)128:7(558).

Cai, G., J. Lin, S. Liu, and A. J. Puppala. 2017. "Characterization of Spatial Variability of CPTU Data in a Liquefaction Site Improved by Vibro-Compaction Method." *KSCE Journal of Civil Engineering* 21 (1): 209–219. https://doi.org/10.1007/s12205-016-0631-1

Cami, B., S. Javankhoshdel, K. K. Phoon, and J. Y. Ching. 2020. "Scale of Fluctuation for Spatially Varying Soils: Estimation Methods and Values." *ASCE-ASME Journal of Risk and Uncertainty in Engineering Systems Part a-Civil Engineering* 6 (4): 03120002. doi/10.1061AJRUA6.0001083.

Campanella, R. G., D. S. Wickremesinghe, and P. K. Robertson. 1987. "Statistical Treatment of Cone Penetrometer Test Data." In *Proceedings, 5th International Conference Application of Statistics and Probability*, Vancouver, 1011–1019.

Cassidy, M. J., M. Uzielli, and Y. H. Tian. 2013. "Probabilistic Combined Loading Failure Envelopes of a Strip Footing on Spatially Variable Soil." *Computers and Geotechnics* 49: 191–205. https://doi.org/10.1016/j.compgeo.2012.10.008.

Ching, J. Y., K. K. Phoon, and S. P. Sung. 2017. "Worst Case Scale of Fluctuation in Basal Heave Analysis Involving Spatially Variable Clays." *Structural Safety* 68:28–42. https://doi.org/10.1016/j.strusafe.2017.05.008.

Ching, J., and T. Schweckendiek. 2021. "State-of-the-art Review of Inherent Variability and Uncertainty in Geotechnical Properties and Models." *ISSMGE Technical Committee* 304: 95–129.

Ching, J. Y., M. Uzielli, K. K. Phoon, and X. J. Xu. 2023. "Characterization of Autocovariance Parameters of Detrended Cone Tip Resistance from a Global CPT Database." *Journal of Geotechnical and Geoenvironmental Engineering* 149 (10): 04023090. https://doi.org/10.1061/JGGEFK.GTENG-11214.

Ching, J. Y., T. J. Wu, A. W. Stuedlein, and T. Bong. 2018. "Estimating Horizontal Scale of Fluctuation with Limited CPT Soundings." *Geoscience Frontiers* 9 (6): 1597–608. https://doi.org/10.1016/j.gsf.2017.11.008.

Dasaka, S. M., and L. M. Zhang. 2012. "Spatial Variability of in Situ Weathered Soil." *Géotechnique* 62 (5): 375–84. https://doi.org/10.1680/geot.8.P.151.3786.

de Gast, T. 2020. "Dykes and Embankments: A Geostatistical Analysis of Soft Terrain." PhD diss., Delft University of Technology.

de Gast, T., M. A. Hicks, A. P. Van den Eijnden, and P. J. Vardon. 2021. "On the Reliability Assessment of a Controlled Dyke Failure." *Géotechnique* 71 (11): 1028–43. https://doi.org/10.1680/jgeot.19.SiP.003

de Gast, T., P. J. Vardon, and M. A. Hicks. 2017. "Estimating Spatial Correlations Under man-Made Structures on Soft Soils." In *Proceedings, 6th International Symposium on Geotechnical Safety and Risk, Denver, Colorado*, edited by Jinsong Huang, Gordon A. Fenton, Limin Zhang, and D. V. Griffiths, 382–389. ASCE Press.

de Gast, T., P. J. Vardon, and M. A. Hicks. 2021. "Assessment of Soil Spatial Variability for Linear Infrastructure Using Cone Penetration Tests." *Géotechnique* 71 (11): 999–1013. https://doi.org/10.1680/jgeot.19.SiP.002

DeGroot, D. J., and G. B. Baecher. 1993. "Estimating Autocovariance of In-Situ Soil Properties." *Journal of Geotechnical Engineering* 119 (1): 147–66. https://doi.org/10.1061/(ASCE)0733-9410(1993)119:1(147)

Fenton, G. A., and D. V. Griffiths. 2002. "Probabilistic Foundation Settlement on Spatially Random Soil." *Journal of Geotechnical and Geoenvironmental Engineering* 128 (5): 381–90. https://doi.org/10.1061/(Asce)1090-0241(2002)128:5(381).

Fenton, G. A., and D. V. Griffiths. 2003. "Bearing-capacity Prediction of Spatially Random c φ Soils." *Canadian Geotechnical Journal* 40 (1): 54–65. https://doi.org/10.1139/t02-086

Fenton, G. A., and D. V. Griffiths. 2008. *Risk Assessment in Geotechnical Engineering*. Vol. 461. New York: Wiley.

Fenton, G. A., and D. V. Griffiths. 2010. "Reliability-based Geotechnical Engineering." In *GeoFlorida 2010: Advances in Analysis, Modeling & Design*, edited by Mohamad H. Hussein, J. Brian Anderson, and William M. Camp, 14–52. https://doi.org/10.1061/41095(365)2.

Fenton, G. A., F. Naghibi, D. Dundas, R. J. Bathurst, and D. V. Griffiths. 2015. "Reliability-based Geotechnical Design in 2014 Canadian Highway Bridge Design Code." *Canadian Geotechnical Journal* 53 (2): 236–51. https://doi.org/10.1139/cgj-2015-0158

Fenton, G. A., and E. H. Vanmarcke. 1990. "Simulation of Random Fields via Local Average Subdivision." *Journal of Engineering Mechanics-Asce* 116 (8): 1733–49. https://doi.org/10.1061/(Asce)0733-9399(1990)116:8(1733).

Firouzianbandpey, S., D. V. Griffiths, L. B. Ibsen, and L. V. Andersen. 2014. "Spatial Correlation Length of Normalized Cone Data in Sand: Case Study in the North of Denmark." *Canadian Geotechnical Journal* 51 (8): 844–57. https://doi.org/10.1139/cgj-2013-0294.

Griffiths, D. V., and G. A. Fenton. 1993. "Seepage Beneath Water Retaining Structures Founded on Spatially Random Soil." *Géotechnique* 43 (4): 577–87. https://doi.org/10.1680/geot.1993.43.4.577.

Griffiths, D. V., and G. A. Fenton. 2001. "Bearing Capacity of Spatially Random Soil: The Undrained Clay Prandtl Problem Revisited." *Géotechnique* 51 (4): 351–9. https://doi.org/10.1680/geot.2001.51.4.351

Griffiths, D. V., and G. A. Fenton. 2004. "Probabilistic Slope Stability Analysis by Finite Elements." *Journal of Geotechnical and Geoenvironmental Engineering* 130 (5): 507–18. https://doi.org/10.1061/(Asce)1090-0241(2004)130:5(507).

Griffiths, D. V., J. S. Huang, and G. A. Fenton. 2009. "Influence of Spatial Variability on Slope Reliability Using

2-D Random Fields." *Journal of Geotechnical and Geoenvironmental Engineering* 135 (10): 1367–78. https://doi.org/10.1061/(Asce)Gt.1943-5606.0000099.

Griffiths, D. V., J. S. Huang, and G. A. Fenton. 2011. "Probabilistic Infinite Slope Analysis." *Computers and Geotechnics* 38 (4): 577–84. https://doi.org/10.1016/j.compgeo.2011.03.006.

Hicks, M. A., J. D. Nuttall, and J. Chen. 2014. "Influence of Heterogeneity on 3D Slope Reliability and Failure Consequence." *Computers and Geotechnics* 61:198–208. https://doi.org/10.1016/j.compgeo.2014.05.004.

Hicks, M. A., and C. Onisiphorou. 2005. "Stochastic Evaluation of Static Liquefaction in a Predominantly Dilative Sand Fill." *Géotechnique* 55 (2): 123–33. https://doi.org/10.1680/geot.2005.55.2.123.

Hicks, M. A., and K. Samy. 2002. "Influence of Heterogeneity on Undrained Clay Slope Stability." *Quarterly Journal of Engineering Geology and Hydrogeology* 35 (1): 41–9. https://doi.org/10.1144/qjegh.35.1.41.

Hicks, M. A., and W. A. Spencer. 2010. "Influence of Heterogeneity on the Reliability and Failure of a Long 3D Slope." *Computers and Geotechnics* 37 (7-8): 948–55. https://doi.org/10.1016/j.compgeo.2010.08.001.

Jaksa, M. B., W. S. Kaggwa, and P. I. Brooker. 1999. "Experimental Evaluation of the Scale of Fluctuation of a Stiff Clay." In *Proceedings, 8th International Conference on Application of Statistics and Probability, Sydney, 1*, edited by R. E. Melchers and M. G. Stewart, 415–422. Balkema: Rotterdam.

Jiang, S. H., J. S. Huang, D. V. Griffiths, and Z. P. Deng. 2022. "Advances in Reliability and Risk Analyses of Slopes in Spatially Variable Soils: A State-of-the-art Review." *Computers and Geotechnics* 141:104498. https://doi.org/10.1016/j.compgeo.2021.104498.

Kim, H. K., and J. C. Santamarina. 2008. "Spatial Variability: Drained and Undrained Deviatoric Load Response." *Géotechnique* 58 (10): 805–14. https://doi.org/10.1680/geot.2008.3724.

Lacasse, S., and F. Nadim. 1997. "Uncertainties in Characterising Soil Properties." *Review of. Publikasjon-Norges Geotekniske Institutt* 201:49–75.

Larsson, S., H. Stille, and L. Olsson. 2005. "On Horizontal Variability in Lime-Cement Columns in Deep Mixing." *Géotechnique* 55 (1): 33–44. https://doi.org/10.1680/geot.2005.55.1.33.

Lees, A., D. A. King, and S. Mimms. 2013. "Palm Jumeirah, Dubai: Cone Penetrometer Testing Data from the Carbonate Sand Fill." *Proceedings of the Institution of Civil Engineers - Geotechnical Engineering* 166 (3): 253–67. https://doi.org/10.1680/geng.10.00070.

Li, Y. J., G. A. Fenton, M. A. Hicks, and N. X. Xu. 2021. "Probabilistic Bearing Capacity Prediction of Square Footings on 3D Spatially Varying Cohesive Soils." *Journal of Geotechnical and Geoenvironmental Engineering* 147 (6): 04021035. https://doi.org/10.1061/(ASCE)GT.1943-5606.0002538.

Li, J. H., J. Huang, M. J. Cassidy, and R. Kelly. 2014. "Spatial Variability of the Soil at the Ballina National Field Test Facility." *Australian Geomechanics* 49 (4): 41–8.

Li, L. J. H., M. Uzielli, and M. J. Cassidy. 2015. "Uncertainty-based Characterization of Piezocone and T-bar Data for the Laminaria Offshore Site." In *Proceedings, 3rd International Symposium on Frontiers in Offshore Geotechnics, ISFOG 2015, Oslo 1*, edited by Vaughan Meyer, 1381–1386. Oslo: CRC Press.

Li, J. H., C. L. Wu, W. Z. Luo, L. W. Sun, and D. J. White. 2022. "An Extended Prandtl Solution for Analytical Modelling of the Bearing Capacity of a Shallow Foundation on a Spatially Variable Undrained Clay." *Géotechnique* 72 (9): 800–9. https://doi.org/10.1680/jgeot.20.P.118.

Liu, Z., ÅM Wist Amdal, J.-S. L. Heureux, S. Lacasse, F. Nadim, and X. Xie. 2019. "Spatial Variability of Medium Dense Sand Deposit." *AIMS Geosciences* 20 (1): 6–30.

Lloret-Cabot, M., G. A. Fenton, and M. A. Hicks. 2014. "On the Estimation of Scale of Fluctuation in Geostatistics." *Georisk: Assessment and Management of Risk for Engineered Systems and Geohazards* 8 (2): 129–40. https://doi.org/10.1080/17499518.2013.871189.

Lloret-Cabot, M., M. A. Hicks, and J. D. Nuttall. 2013. "Investigating the Scales of Fluctuation of an Artificial Sand Island." In *Installation Effects in Geotechnical Engineering*, edited by Michael A. Hicks, Jelke Dijkstra, Marti Lloret-Cabot, and Minna Karstunen, 192–197. Rotterdam; CRC Press.

Lloret-Cabot, M., M. A. Hicks, and A. P. van den Eijnden. 2012. "Investigation of the Reduction in Uncertainty due to Soil Variability When Conditioning a Random Field Using Kriging." *Géotechnique Letters* 2 (3): 123–7. https://doi.org/10.1680/geolett.12.00022.

Monforte, Ll. 2024. "Inherent and CPTu-Measured Scale of Fluctuation of Undrained Geomaterials: A Numerical Perspective." In *Proceedings, 7th International Conference on Geotechnical and Geophysical Site Characterization*, 162–190. Barcelona: CIMNE.

Onyejekwe, S., X. Kang, and L. Ge. 2016. "Evaluation of the Scale of Fluctuation of Geotechnical Parameters by Autocorrelation Function and Semivariogram Function." *Engineering Geology* 214:43–9. https://doi.org/10.1016/j.enggeo.2016.09.014.

Phoon, K. K. 2008. *Reliability-based Design in Geotechnical Engineering: Computations and Applications*. London: CRC Press.

Phoon, K. K., and F. H. Kulhawy. 1999. "Characterization of Geotechnical Variability." *Canadian Geotechnical Journal* 36 (4): 612–24. https://doi.org/10.1139/t99-038.

Pieczyńska-Kozłowska, J. M., M. Chwała, and W. Puła. 2023. "Worst-case Effect in Bearing Capacity of Spread Foundations Considering Safety Factors and Anisotropy in Soil Spatial Variability." *Georisk: Assessment and Management of Risk for Engineered Systems and Geohazards* 17 (2): 330–45. https://doi.org/10.1080/17499518.2022.2046786

Pieczyńska-Kozłowska, J., and G. Vessia. 2022. "Spatially Variable Soils Affecting Geotechnical Strip Foundation Design." *Journal of Rock Mechanics and Geotechnical Engineering* 14 (3): 886–95. https://doi.org/10.1016/j.jrmge.2021.10.010

Popescu, R., G. Deodatis, and A. Nobahar. 2005. "Effects of Random Heterogeneity of Soil Properties on Bearing Capacity." *Probabilistic Engineering Mechanics* 20 (4): 324–41. https://doi.org/10.1016/j.probengmech.2005.06.003.

Poulos, H. G. 2018. "A Review of Geological and Geotechnical Features of Some Middle Eastern Countries." *Innovative*

Infrastructure Solutions 3 (1): 1–18. https://doi.org/10.1007/s41062-018-0158-z.

Renton-Rose, D. G., G. C. Bunce, and D. W. Finlay. 2000. "Vibro-replacement for Industrial Plant on Reclaimed Land Bahrain." *Géotechnique* 50 (6): 727–37. https://doi.org/10.1680/geot.2000.50.6.727.

Schorr, J., R. Cudmani, and K. Nübel. 2023. "Interpretation of Field Tests Using geo-Statistics and Kriging to Assess the Deep Vibratory Compaction of the Dike A21, Diavik Diamond Mine." *Acta Geotechnica* 18 (3): 1391–405. https://doi.org/10.1007/s11440-022-01675-6

Slocombe, B. C., A. L. Bell, and J. I. Baez. 2000. "The Densification of Granular Soils Using Vibro Methods." *Géotechnique* 50 (6): 715–25. https://doi.org/10.1680/geot.2000.50.6.715.

Stuedlein, A. W., S. L. Kramer, P. Arduino, and R. D. Holtz. 2012. "Geotechnical Characterization and Random Field Modeling of Desiccated Clay." *Journal of Geotechnical and Geoenvironmental Engineering* 138 (11): 1301–13. https://doi.org/10.1061/(Asce)Gt.1943-5606.0000723.

Uzielli, M., S. Lacasse, F. Nadim, and K. K. Phoon. 2007. "Soil Variability Analysis for Geotechnical Practice." *Characterisation and Engineering Properties of Natural Soils* 3 (4): 1653–752.

Uzielli, M., G. Vannucchi, and K. K. Phoon. 2005. "Random Field Characterisation of Stress-Nomalised Cone Penetration Testing Parameters." *Géotechnique* 55 (1): 3–20. https://doi.org/10.1680/geot.2005.55.1.3

Vanmarcke, E. 1983. "*Random Fields: Analysis and Synthesis*." Review of. *Cambridge*.

Vessia, G., C. Cherubini, J. Pieczyńska, and W. Puła. 2009. "Application of Random Finite Element Method to Bearing Capacity Design of Strip Footing." *Journal of GeoEngineering* 4 (3): 103–12.

Wackernagel, H. 2003. *Multivariate Geostatistics: An Introduction with Applications*. Berlin: Springer Science & Business Media.

Wickremesinghe, D., and R. G. Campanella. 2020. "Scale of Fluctuation as a Descriptor of Soil Variability." *Proceedings, Probabilistic Methods in Geotechnical Engineering, Canberra*, edited by K. S. Li and S.-C. R. Lo, 233–239. London: CRC Press. https://doi.org/10.1201/9781003077749-22

Zhai, S. J., G. Y. Du, C. H. Gao, S. Y. Liu, T. Peng, and H. He. 2024. "Effect of Vibratory Probe Compaction Method on Bearing Capacity of Loess Investigated via Random Finite Element Analysis." *Soil Dynamics and Earthquake Engineering* 186:108914. https://doi.org/10.1016/j.soildyn.2024.108914.

Zhang, J. Z., K. K. Phoon, D. M. Zhang, H. W. Huang, and C. Tang. 2021. "Novel Approach to Estimate Vertical Scale of Fluctuation Based on CPT Data Using Convolutional Neural Networks." *Engineering Geology* 294:106342. https://doi.org/10.1016/j.enggeo.2021.106342.

Zhang, Jin-Zhang, D.-M. Zhang, H.-W. Huang, K. K. Phoon, C. Tang, and G. Li. 2022. "Hybrid Machine Learning Model with Random Field and Limited CPT Data to Quantify Horizontal Scale of Fluctuation of Soil Spatial Variability." *Acta Geotechnica* 17: 1129–1145.

Appendix

For completeness, the spatial statistics corresponding to sleeve friction are tabulated below.

Table A1. Vertical and horizontal correlation lengths for sleeve friction at trial test site A.

	Pre-CPT		Post-CPT	
Trial site A	θ_v: (m)	θ_h: (m)	θ_v: (m)	θ_h: (m)
A1	0.61	–	0.36	–
A2	0.83	–	0.28	–
A3	0.81	–	0.40	–
A4	0.69	–	0.21	–
T-A	–	–	0.43	–
Average	**0.74**	**40.30**	**0.34**	**5.70**
σ^2	**0.01**	**–**	**0.01**	**–**
CoV	**0.12**	**–**	**0.24**	**–**

Note: μ, mean; σ^2, variance; CoV, coefficient of variation and θ, correlation length.

Table A2. Vertical and horizontal correlation lengths for sleeve friction at trial test site B.

	Pre-CPT		Post-CPT	
Trial site B	θ_v: (m)	θ_h: (m)	θ_v: (m)	θ_h: (m)
B1	0.71	–	0.36	–
B2	1.28	–	0.74	–
B3	0.76	–	0.56	–
B4	0.91	–	0.53	–
T-B	–	–	0.44	–
Average	**0.92**	**52.40**	**0.53**	**19.40**
σ^2	**0.05**	**–**	**0.02**	**–**
CoV	**0.24**	**–**	**0.24**	**–**

Note: μ, mean; σ^2, variance; CoV, coefficient of variation and θ, correlation length.

Table A3. Vertical and horizontal correlation lengths for sleeve friction at trial test site C.

	Pre-CPT		Post-CPT	
Trial site C	θ_v: (m)	θ_h: (m)	θ_v: (m)	θ_h: (m)
C1	2.46	–	0.42	–
C2	2.19	–	0.35	–
C3	0.62	–	0.31	-
C4	0.47	–	0.28	–
C5	2.32	–	0.25	–
T-C	–	–	0.81	–
Average	**1.61**	**17.00**	**0.40**	**13.40**
σ^2	**0.77**	**–**	**0.04**	**–**
CoV	**0.54**	**–**	**0.47**	**–**

Note: μ, mean; σ^2, variance; CoV, coefficient of variation and θ, correlation length.